

Hannes König, B. Eng.

# **A novel streptavidin-based affinity matrix for the immobilization of strep-tagged enzymes**

## **MASTER'S THESIS**

to achieve the university degree of

Master of Science

Master's degree programme:

Biotechnology

submitted to

**Graz University of Technology**

### **Supervisor**

Univ.-Prof. Dipl.-Ing. Dr. techn. Bernd Nidetzky  
Institute of Biotechnology and Biochemical Engineering

second supervisor

Dipl.-Ing. Dr. techn. Alexander Gutmann

## AFFIDAVIT

I declare that I have authored this thesis independently, that I have not used other than the declared sources/resources, and that I have explicitly indicated all material which has been quoted either literally or by content from the sources used. The text document uploaded to TUGRAZonline is identical to the present master's thesis.

23.02.2021



---

Date, Signature

## Content

Content .....	1
Danksagung .....	4
Kurzfassung .....	5
Abstract .....	7
Abbreviations .....	8
1 Introduction .....	9
1.1 Applications of Z <sub>basic2</sub> as silica binding module .....	10
1.2 Current examples of the generation of streptavidin-based affinity matrix .....	12
1.3 Current application of enzyme immobilization using <i>strep-tag</i> II .....	13
1.4 Description of the “bio-coupled” protein-based affinity matrix .....	13
1.5 Insoluble support and attachment of proteins via Z <sub>basic2</sub> .....	14
1.6 Expression of SAV in <i>E. coli</i> .....	16
1.7 The interaction of SAV and <i>strep-tag</i> II .....	17
1.8 Description of the enzymatic model reaction .....	18
2 Objectives .....	20
3 Material and methods .....	21
3.1 Expression of recombinant SAV .....	21
3.1.1 Cytoplasmic expression of recombinant Z <sub>basic2</sub> -SAV in <i>E. coli</i> .....	21
3.1.2 Expression of Z <sub>basic2</sub> -SAV in other <i>E. coli</i> strains .....	22
3.1.3 Periplasmic expression Z <sub>basic2</sub> -SAV with the signal sequence OmpA .....	23

---

3.2	Protein purification of recombinant SAV .....	24
3.2.1	Development of standard purification protocol of SAV with Fractogel® .....	25
3.2.2	Column purification of SAV with Äkta FPLC .....	26
3.3	Determination of purity using SDS-PAGE.....	27
3.4	Determination of maximum protein loading of Fractogel® .....	27
3.5	Determination of maximum protein loading of underivatized silica beads .....	28
3.6	Immobilization of <i>OsCGT</i> and <i>GmSuSy</i> on SAV affinity matrix.....	29
3.7	Regeneration of SAV affinity matrix.....	30
4	Results and Discussion.....	31
4.1	Cytoplasmic expression of recombinant SAV .....	31
4.2	Periplasmic expression of $Z_{\text{basic2-SAV}}$ .....	33
4.3	Development of a purification procedure of $Z_{\text{basic2-SAV}}$ .....	36
4.4	Characterization of $Z_{\text{basic2-SAV}}$ affinity matrix.....	38
4.4.1	Maximum $Z_{\text{basic2-SAV}}$ loading capacity of different carriers .....	38
4.4.2	$Z_{\text{basic2-SAV}}$ immobilized on underivatized silica beads .....	39
4.4.3	Elution of protein and protein recovery .....	40
4.4.4	Regeneration of the $Z_{\text{basic2-SAV}}$ -silica beads affinity matrix .....	41
4.5	Application of affinity matrix for immobilization and enzyme catalysis.....	42
4.5.1	Enzymatic catalysis with immobilized enzyme.....	42
4.5.2	Analysis of reaction solutions fractions .....	43
4.5.3	Remaining enzyme activity and recovery .....	44
4.5.4	Binding strength of <i>strep-tag II</i> and $Z_{\text{basic2-SAV}}$ .....	45

5 Conclusion and Outlook .....47

6 References .....49

7 Appendix.....55

## Danksagung

Ich möchte mich zu aller Erst bei Prof. Dr. Bernd Nidetzky für die Möglichkeit und die Betreuung bedanken meine Masterarbeit am Institut für Biotechnologie durchzuführen. Mein besonderer Dank gilt Dr. Alexander Gutmann für die umfangreiche Betreuung im Labor und während der Erstellung meiner Masterarbeit. Er hatte bei Problemen und Fragen immer ein offenes Ohr. Mein Dank gilt auch den Mitarbeitern und Studenten des Instituts für Biotechnologie die mir bei Fragen mit Rat und Tat zur Seite standen.

Ich möchte mich außerdem bei meinen Eltern und meinem Bruder für Ihre Unterstützung und Möglichkeit mein Masterstudium durchzuführen bedanken.

## Kurzfassung

Häufig werden Biokatalysatoren für industrielle Prozesse als unerschwinglich angesehen, sofern die Enzyme nicht wiederverwendet werden können. Die Enzymimmobilisierung an festen Trägern erleichtert deren Rückgewinnung und Wiederverwendung erheblich. Idealerweise kann auch das meist teure Trägermaterial wiederverwendet werden. In dieser Arbeit wurde die reversible Enzymbindung durch starke nichtkovalente Wechselwirkung untersucht. Enzyme mit *strep-tag* II wurden selektiv auf einem Streptavidin-Trägermaterial unter milden Bedingungen immobilisiert, welche aus der Strep-tag-Affinitätschromatographie bekannt sind. Der Streptavidinträger selbst wurde durch die Wechselwirkung eines positiv geladenen  $Z_{\text{basic2}}$ -Tags und eines Kationenaustauscherharz (Fractogel® EMD SO3- (M)) oder unmodifizierte Quarzglasperlen (Trisoperl) hergestellt. Beide Immobilisierungsschritte waren reversibel, um die Rückgewinnung des Trägermaterials mit oder ohne gebundenem Streptavidin zu ermöglichen. Die Expression des toxischen  $Z_{\text{basic2}}$ -markierten Streptavidins in *Escherichia coli* und seine selektive Immobilisierung aus unbehandeltem Zellextrakt an Fractogel®-Harz wurden optimiert. Die  $Z_{\text{basic2}}$ -Streptavidin-Bindungskapazität von Fractogel® und Trisoperl betrug 292 bzw. 54 mg pro g trockenem Trägermaterial. Mit Streptavidin beschichtetes Trisoperl wurde verwendet, um eine C-Glucosyltransferase aus Reis (*Oryza sativa*, OsCGT) und eine Saccharosesynthase aus Sojabohnen (*Glycine max*, GmSuSy) gemeinsam zu immobilisieren. In der Modellreaktion katalysierte OsCGT die Synthese von Nothofagin durch C-Glucosylierung von Phloretin. GmSuSy wurde zur In-situ-Regeneration des Glucosedonors UDP-Glucose aus UDP und Saccharose verwendet. Obwohl ein gewisses Auswaschen beobachtet wurde, konnte das Trägermaterial für acht aufeinanderfolgende Zyklen wiederverwendet werden. Ein Beweis des Prinzips der Tandem-Immobilisierungsstrategie wurde erbracht. Zur Anwendung des Systems sollte die Expression

von Z<sub>basic2</sub>-Streptavidin weiter verbessert und modifizierte Versionen des Streptavidin-Affinitätssystems mit verbesserter Bindungsstärke getestet werden.

## Abstract

Frequently high costs of biocatalysts are considered prohibitive for industrial processes unless enzymes can be reused. Enzyme immobilization to solid carriers strongly facilitates their recovery and reuse. Ideally also the typically costly carrier can be reused. In this work reversible enzyme attachment by strong noncovalent interaction was investigated. *Strep-tag II* containing proteins were selectively immobilized on a streptavidin containing carrier under mild conditions well known from Strep-tag affinity chromatography. The streptavidin carrier itself was produced by attachment through a fused positively charged  $Z_{\text{basic2}}$  tag to a strong cation exchange resin (Fractogel® EMD  $\text{SO}_3^-$  (M)) or unmodified silica glass (Trisoperl) beads. Both immobilization steps were reversible to allow recovery of resin with or without attached streptavidin. Expression of toxic  $Z_{\text{basic2}}$ -tagged streptavidin in *Escherichia coli* and its selective immobilization from crude cell extract to the Fractogel®™ resin were optimized. The  $Z_{\text{basic2}}$ -streptavidin binding capacity on Fractogel®™ and Trisoperl were 292 and 54 mg per g dry carrier, respectively. Streptavidin coated Trisoperl was used to co-immobilize a *C*-glucosyltransferase from rice (*Oryza sativa*, *OsCGT*) and a sucrose synthase from soybean (*Glycine max*, *GmSuSy*). In the model reaction *OsCGT* catalyzed synthesis of nothofagin by *C*-glucosylation of phloretin. *GmSuSy* was used for in situ regeneration of the glucose donor UDP-glucose from UDP and sucrose. Although some wash-out was observed, the carrier could be reused for eight consecutive cycles. A proof of principle of the tandem immobilization strategy was obtained. For synthetic application of the system expression of  $Z_{\text{basic2}}$ -streptavidin should be further improved and modified versions of the streptavidin affinity system with improved binding strength should be tested.

## Abbreviations

ACN	acetonitrile
CV	column volume
<i>E. coli</i>	<i>Escherichia coli</i>
GmSuSy	sucrose synthase from soybean ( <i>Glycine max</i> )
HABA	2-(4-hydroxyphenylazo)benzoic acid
HPLC	high performance liquid chromatography
$K_d$	dissociation constant
LB	lysogeny broth
MTP	modified tryptone-phosphate
OsCGT	<i>C</i> -glucosyltransferase from rice ( <i>Oryza sativa</i> )
PPG	polypropylene glycol
$pK_a$	negative decadic logarithm of the acid dissociation constant
SAV	streptavidin
<i>strep-tag</i> (II)	eight-amino-acid peptide affinity tag
TB	terrific broth
TEV	tobacco etch virus
UDP	uridine diphosphate
Z <sub>basic2</sub>	protein tag obtained from the B domain of <i>staphylococcal</i> protein A
IPTG	isopropyl- $\beta$ -D-thiogalactopyranoside

# 1 Introduction

Immobilization of enzymes typically causes insolubilization of the catalyst and allows simple separation from the reaction solution, which can significantly reduce costs of enzyme driven processes. Attached enzymes can exhibit enhanced rigidity and stability, whereby stabilization is the most frequent target of immobilization strategies [1]. Other possible improved properties include enzyme activity, selectivity and specificity [1, 2]. The general mechanisms of immobilization can be categorized into covalent or non-covalent attachment to a support, entrapment and cross-linking [3, 4]. Non-covalent adsorption of enzyme to a support can involve combinations of physical (e.g. hydrogen bonds and van-der-Waal forces), hydrophobic and electrostatic interactions [4, 5]. A non-covalent immobilization of enzymes creates the possibility of regeneration of the in most cases costly support and/or catalyst [6].

The streptavidin-biotin interaction got of interest, because of the very tight non-covalent binding of vitamin H (biotin) with a dissociation constant of  $K_d = 4 \times 10^{-14}$  M [7]. Thereby it is representing one of the strongest binding affinities in nature. Streptavidin (SAV) itself exhibits a high stability against elevated temperatures, extremes of pH and denaturants [8]. This makes SAV as a ligand to a versatile tool in affinity-based applications, like purification and immobilization. For the application as affinity ligand in a bio-coupled affinity-matrix considerations about solid material on which SAV will be immobilized have to be done. The support material should be chemical and physical stable, having a great capacity of absorption of the target ligand and low non-specific adsorptions. A strong interaction mode of the affinity ligand and support have to be used to prevent leaching of the ligand during operation. The protein structure should also include a spacer between the surface of the support and the ligand to ensure accessibility of SAV binding pocket and a favorable orientation. Interaction with other proteins should be minimal [9].

For this purpose, a recombinantly expressed SAV with fused  $Z_{\text{basic2}}$ -tag was utilized in this study in combination with underivatized silica beads (controlled poor glass). The  $Z_{\text{basic2}}$ -tag served as silica binding module. The generated affinity matrix was applied for the immobilization of strep-tagged enzymes and enzymatic syntheses of nothofagin was used as a model reaction.

## 1.1 Applications of $Z_{\text{basic2}}$ as silica binding module

The application of the cationic binding module  $Z_{\text{basic2}}$  can be advantageous as it involves a strongly but reversible binding of the tagged enzyme to anionic supports by electrostatic interactions in an oriented way [6, 13, 15, 16]. Bolivar et al. immobilized D-Amino acid oxidase (*Trigonopsis variabilis*, *TvDAO*) and sucrose phosphorylase (*Leuconostoc mesenteroides*, *LmSPase*) on anionic supports (Fractogel® and Sepabeads) [6] and controlled poor glass (underivatized silica beads) [13] under mild pH conditions. The enzymatic activity upon attachment remained similar in comparison to theoretically activity of free enzyme at low protein loadings. Consequently, a favorable orientation of the enzymes was concluded. The immobilization with  $Z_{\text{basic2}}$ -tag was achieved directly from crude cell extract in a highly selective manner at high protein loadings. Thus, opening the opportunity of one-step purification and immobilization for  $Z_{\text{basic2}}$ -tagged enzymes [6, 13]. These properties of  $Z_{\text{basic2}}$  should be beneficial for the immobilization of  $Z_{\text{basic2}}$ -SAV on silica and anionic supports and boost the applicability of generated the  $Z_{\text{basic2}}$ -SAV affinity matrix.

The accessibility of carrier surface is important to reach a feasible immobilization yield (offered protein/activity versus bound protein/activity) [6, 39]. A homogenous distribution on outer and inner surface was shown for *TvDAO* after immobilization via  $Z_{\text{basic2}}$ -interaction on controlled pore glass and two mesoporous silica materials (MSU-VLP, MSU-F) by confocal laser scanning microscopy [14]. Even for MSU-F with smallest pore size of 17 nm compared to

molecular dimension of the enzyme (10 nm x 7 nm x 4.5 nm) high loading was possible. The controlled pore glass used in this thesis with 161.2 nm pore size will be investigated for the immobilization of  $Z_{\text{basic2}}$ -SAV.

Comparing multipoint covalent attachment of His\_*Lm*SPase to epoxy-processed Sepabeads to non-covalent immobilization of  $Z_{\text{basic2}}$ -*Lm*SPase revealed similar efficiency in synthesis of glucosyl glycerol [40]. From this observation it was concluded that it is preferable to use the  $Z_{\text{basic2}}$  non-covalent attachment with the possibility of immobilization from crude enzyme extract and regeneration of the carrier. This simplifies the generation of active insoluble catalyst based on  $Z_{\text{basic2}}$  and shows another example of one-step purification-immobilization approach. The continuous production of glucosyl glycerol with  $Z_{\text{basic2}}$ -*Lm*SPase was achieved in a microstructured flowreactor with  $\gamma$ -aluminium oxide wash-coat layer in the same study [40]. The approximately operational half-life in this case was around 10 days and a continuous production over 16 days was shown. These findings imply high stability and productivity in a continuous reaction approach using  $Z_{\text{basic2}}$ -tag.

Different co-immobilization studies were also conducted using  $Z_{\text{basic2}}$  as binding module. *Ti*DAO and catalase (*Bordetella pertussis*) were co-immobilized on different mesoporous silica materials with varying pore structure to analyze the influence on enzyme loading and immobilization yield [39]. A uniform pore structure of the silica materials was identified beneficial for the oxidation of D-methionine and could be important in general for O<sub>2</sub> dependent reactions including enzyme immobilizates. Three glycoside phosphorylases carrying  $Z_{\text{basic2}}$ -tag were immobilized on macro-porous polymethacrylate particles for the efficient syntheses of cello-oligosaccharides and integrated re-use as another example [41]. In a co-immobilization study via  $Z_{\text{basic}}$  Valikhani et. al immobilized Cytochrome P450 BM3 and glucose dehydrogenase (from *Bacillus mageterium*) in controllable manner, a high recyclability and increased robustness [42].

These different applications emphasize the use of  $Z_{\text{basic2}}$  as variable but controllable binding module for the immobilization of recombinant SAV and the use in continues enzymatic reactions.

## 1.2 Current examples of the generation of streptavidin-based affinity matrix

The generation of a SAV-based affinity matrix can involve different ways of preparation in terms of the used attachment approach. Wu et al. [10] immobilized an engineered SAV containing galactose binding domain (from *Lumbricus terrestris*) to allow reversible fusion to agarose beads. The resulting matrix was applied for purification (in column format) of streptavidin binding peptide (SBP) tagged  $\beta$ -lactamase, biotinylated maltose binding protein (one biotin) and biotinylated BSA (12 biotins). Over a period of six months no obvious decrease of column performance in binding biotinylated BSA were found implying strong stability of the derived matrix. This stability was mainly attributed to the avidity effect due to tetrameric structure of SAV. Additionally, the purification performance was compared between a matrix built of SAV subsequently purified and SAV immobilized directly from crude cell extract. The performance was similar implying the potential simplification of the generation of the affinity matrix by skipping the purification of SAV.

Wu et al. [11] used dextran-binding domain fused to SAV to immobilize on Sephadex® matrix directly from cell extract. The capture efficiency (based on assumption that one tetrameric streptavidin binds two biotinylated BSA molecules) of the bio-coupled affinity matrix was compared to chemically immobilized SAV using activated affinity gel as matrix. The bio-coupled matrix showed a capture efficiency of 73.0 % for fully saturated matrix and 75.8 % for half saturated matrix (% of applied biotinylated BSA which is bound) in contrast to 48.9 % using

the chemically coupled matrix. They attributed this to the mainly randomized orientation of SAV when coupled chemically resulting in a reduced availability of STV binding pockets through steric hindrances.

### 1.3 Current application of enzyme immobilization using *strep-tag II*

Due to the low interaction of *strep-tag II* to protein function, the immobilization of strep-tagged enzyme could be a convenient way of immobilization. Johar et al. [12] immobilized CALB (Lipase B from *Candida antarctica*) carrying a *strep-tag II* on *Strep-Tactin*®. The enzymatic activity is decreasing when comparing free enzyme and immobilized enzyme. The catalytic rate constant ( $k_{\text{cat}}$ ) is reduced from  $70.7 \pm 11.3 \text{ s}^{-1}$  to  $6.53 \pm 0.767 \text{ s}^{-1}$  upon immobilization whereas the apparent  $K_M$  was not significantly affected. Possible explanations including additional interactions of the enzyme with the support or protein-protein interactions resulting in conformational changes of the enzyme. Anyway, the recovery from the support was possible. Therefore, the conformation change appears to be slow or reversible. Enhanced stability of CALB was not occurring in contrast to other reported results with other immobilization methods.

### 1.4 Description of the “bio-coupled” protein-based affinity matrix

In this study following approaches were made: 1) Generation of “bio-coupled” affinity matrix using recombinant SAV and a suitable carrier (Fractogel® and underivatized silica beads) and 2) Application of immobilized strep-tagged enzymes for enzymatic conversions. For the enzymatic catalysis only underivatized silica beads with SAV immobilized was used. The assembly and application of the protein-based affinity matrix included three steps: (A) Immobilization of recombinantly expressed  $Z_{\text{basic2\_SAV}}$  at neutral pH via the positively charged binding-domain  $Z_{\text{basic2}}$  to the negatively charged surface of the underivatized silica beads. (B)

Immobilization of the monomeric *C*-glucosyltransferase from rice (*Oryza sativa*; *OsCGT*) and tetrameric sucrose synthase from soybean (*Glycin max*; *GmSuSy*) via fused affinity tag *strep-tag II* and (C) In a cascade reaction the bound *OsCGT* catalyzes the *C*-glucosylation of phloretin using UDP-glucose as glucosyl donor. The synthesis is combined with the regeneration of UDP-glucose from sucrose by *GmSuSy* (reaction see 1.8).

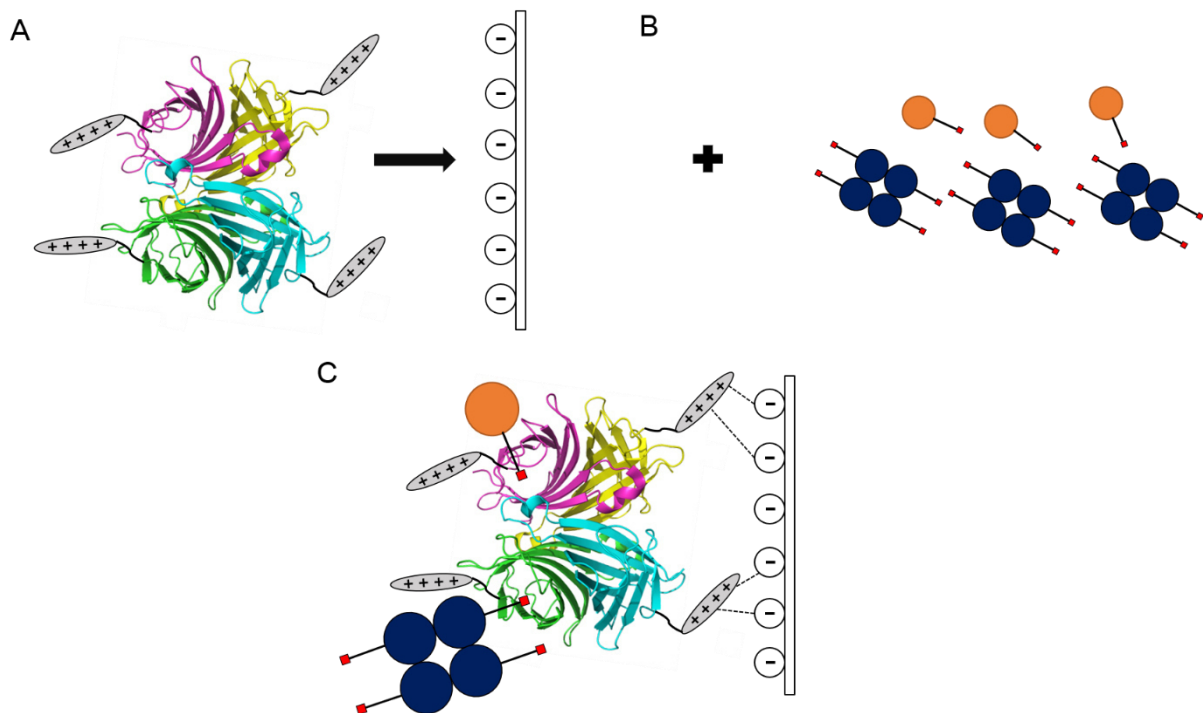


**Fig. 1-1: Schematic representation of the protein-based affinity matrix and proposed immobilization of enzymes containing *strep-tag II*.** (A): Binding of the affinity ligand tetrameric SAV via fused positively charged Z<sub>basic2</sub>-binding domain (grey) to negatively charged silanol groups at the surface of underivatized silica beads at neutral pH. (B): Applying of monomeric *C*-glucosyltransferase from rice (*Oryza sativa*, orange) and homotetrameric sucrose synthase from soybean (*Glycin max*, blue). (C): Proposed binding of the enzymes via small affinity-tag *strep-tag II* (red quadrat).

## 1.5 Insoluble support and attachment of proteins via Z<sub>basic2</sub>

Silica materials as suitable inorganic supports can be applied in a wide range of immobilization applications [13, 14]. For the oriented immobilization of Z<sub>basic2</sub>-SAV on such support's considerations in terms of isoelectric point of the binding module and the immobilization support have to be made. At neutral pH the common silanol group (Si-OH) of silica-based

materials is deprotonated, having a  $pK_a$  value in the range of  $\sim 6-7$  and is forming a negatively net charge. The character of a weak cation exchanger is generated [13]. The  $pI$  of the  $Z_{\text{basic2-}}$  tag, determined by sequence, is 10.5 and therefore  $Z_{\text{basic2-}}$  has a highly positive net charge at neutral pH. Electrostatic interactions probably promote the oriented immobilization of  $Z_{\text{basic2-}}$  SAV [13, 15, 16]. Next to this interaction hydrophobic adsorption can occur due to hydrophobic character of siloxanes in the silica support [13].

Another insoluble support applied for the binding of  $Z_{\text{basic2-}}$  SAV was Fractogel® EMD  $\text{SO}_3^-$  (M). The sulfoisobutyl-groups of the strong cation exchanger having a  $pK_a$  of  $< 1$  are carrying strongly negative charges at neutral pH. Wiesbauer et. al. [6] showed successful immobilization of one dimeric as well as one monomeric enzyme via  $Z_{\text{basic2-}}$  module on Fractogel® with favorable orientation and pointed out, that the method is basically applicable to monomeric and multimeric proteins.

The pore size could be another critical parameter for the attachment of  $Z_{\text{basic2-}}$  SAV, as it should be at least five times greater than the size of the ligand to ensure accessibility for the catalysts immobilized in the second step [9]. Furthermore, the pore size, porosity and the particle size define the accessible surface area for attachment of the protein.

**Tab. 1-1: Overview of key features of the insoluble support materials Fractogel® EMD  $\text{SO}_3^-$  (M) and Trisoperl glass beads (underivatized silica beads). n.a. not applicable**

Property	Fractogel®™ EMD $\text{SO}_3^-$ (M)	Trisoperl (glass beads) <sup>1</sup>
Character	Strong cation exchanger	Weak cation exchanger
Functional group	Sulfoisobutyl-group $-\text{C}(\text{CH}_3)_2-\text{CH}_2-\text{SO}_3^-$	Slightly acidic silanol groups Si-OH
$pK_a$	$< 1$	$\sim 6-7$
Matrix material	cross-linked polymethacrylate resin	underivatized silica

Property	Fractogel®™ EMD SO <sub>3</sub> <sup>-</sup> (M)	Trisoperl (glass beads) <sup>1</sup>
Structure	“tentacle” structure	porous spherical beads
Particle size [μm]	40 – 90	50 – 100
Pore size [nm]	80	161.2
Binding capacity [mL <sub>suspension</sub> <sup>-1</sup> ]	130 mg lysozyme (according to manufacturer)	-

<sup>1</sup> data from [13].

## 1.6 Expression of SAV in *E. coli*

The expression of SAV in *E. coli* is challenging, because of its toxicity upon binding of the essential growth vitamin biotin and other biotinylated bacterial proteins [17]. A tightly regulated expression is inevitable in sense of optimizing expression yields. The tendency of *E. coli* to form inclusion bodies of SAV lead to involvement of refolding procedures in most expression protocols [17–19]. Humbert et al. [17] applied the *E. coli* strain BL21(DE3) pLysS as expression host in combination with a pET11-plasmid, which allowed for the suppression of basal toxic expression of SAV prior induction. The pLysS plasmid of the strain provides T7-lysozym which can inhibit T7-polymerase before induction [20]. Next to optimized pH, glucose concentration and time of induction this features enabled expression levels of up to 230 mg L<sup>-1</sup> culture media of functional SAV after a single step of de- and-renaturation [17].

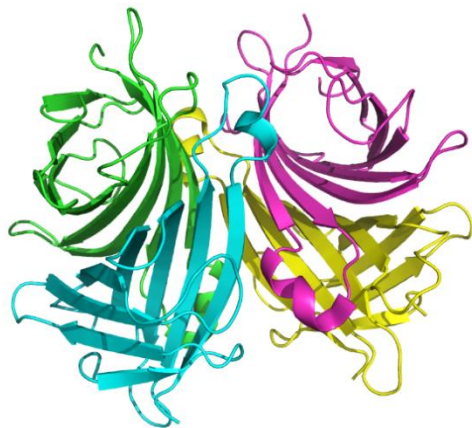
Another possible way to overcome the toxicity of SAV is the guided translocation to the periplasmic space of *E. coli* using the signal peptide for outer membrane protein A (*OmpA*) [21]. The signal sequence (MKKTAIAIAVALAGFATVAQA) is fused to the sequence of the protein of interest and a premature protein is expressed in the cytoplasm. After that the signal

sequence is guiding the translocation into periplasmic space and is cleaved resulting in the mature protein [22].

### 1.7 The interaction of SAV and *strep-tag II*

SAV is originally derived from *Streptomyces avidinii* and consists of four identical subunits, whereby each is forming an antiparallel  $\beta$ -barrel [23]. Each of the subunits contains a binding pocket for one molecule of biotin. Commercially available SAV named core SAV is a proteolytically truncated form of SAV covering the sequence from Ala<sup>13</sup> or Glu<sup>14</sup> to Ala<sup>138</sup> or Ser<sup>139</sup>, respectively [18, 24]. In comparison to the mature protein, which is secreted from *Streptomyces*, it exhibits increased solubility and resistance to degradation [18]. It is also highly stable against elevated temperatures up to 75 °C and additives like salts and detergent [18, 24, 25].

(A)



(B)

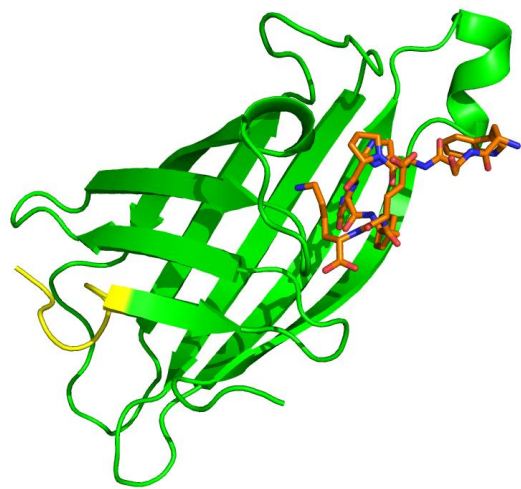


**Fig. 1-2: 3-D structure of recombinant core SAV in cartoon presentation (PDB 1RSU [26]) (A): SAV tetramer showing the arrangement of the four subunits (green, cyan, pink, yellow) (B): SAV monomer with bound *strep-tag II* (represented as orange sticks). Position of fused Z<sub>basic2</sub>-domain is marked in yellow. The figures were generated with PyMOL program (The PyMOL Molecular Graphics System, Version 2.3.2 Schrödinger, LLC)**

The eight-amino-acid artificial peptide *strep-tag* (sequence: WRHPQFGG) which binds tightly to core SAV was derived from a genetic random library [24]. The tag was originally engineered

for the detection and purification of recombinantly expressed proteins applying its competitive binding with biotin to SAV [26]. The binding includes the formation of hydrogen bonds, incorporation of hydrogen-bonded water molecules and forming of a salt bridge of the free carboxylate group of *strep-tag* and Arg 84 of SAV [21, 26]. To overcome the limitation of the fusion to the C-terminus of target proteins the *strep-tag* II (sequence: WSHPQFEK) was developed which exhibits an affinity to core SAV of approximately  $K_d = 13 \mu\text{M}$  [26]. Because the shift in the sequence decreased the affinity of the *strep-tag* II, core SAV itself was engineered. The dissociation constant of *strep-tag* II was increased to an approximately  $K_d$  of  $1 \mu\text{M}$  upon introduction of *Tactin*<sup>®</sup> mutation (mutation of flexible loop in core SAV) [21]. The affinity constant for purification in general is recommend to be in the range of  $1 \mu\text{M} - 1 \text{nM}$  [9]. The accomplished affinity of *strep-tag* II and *Strep-Tactin*<sup>®</sup> therefore should also enable the immobilization of enzymes using core SAV.

## 1.8 Description of the enzymatic model reaction

For enzymatic cascade reactions co-immobilization of enzymes by affinity adsorption tends to be kinetically favorable. The diffusion distance of the product of the first reaction to the second enzyme is minimized and the second enzyme can immediately access the first product in relatively high concentration. Consequently, the same immobilization mechanism is mandatory and the enzyme with weaker stability is determining the shelf-life of the setup catalyst [1]. The substrate, which is consumed faster, could suffer from diffusion limitations, which has to be considered in the reaction design.

By keeping this challenges in mind the coupled enzymatic synthesis of nothofagin, a biologically active antioxidant aryl C-glycoside found in rooibos, with regeneration of the glucosyl donor was studied as model reaction [27]. C-glycosylation of the dihydrochalcone

phloretin by *OsCGT* results in formation of nothofagin. The glucosyl donor UDP-glucose is regenerated by *GmSuSy* catalyzing the reaction of UDP and sucrose[27].

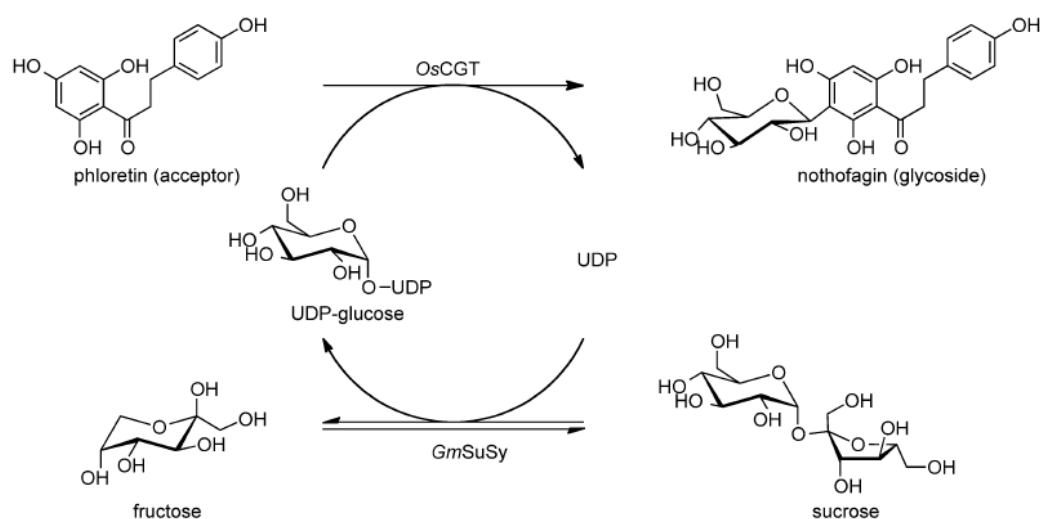


**Fig. 1-3: Combined synthesis of nothofagin** by *OsCGT* catalyzing the *C*-glucosylation of phloretin using UDP-glucose as glucosyl donor with regeneration of UDP-glucose from sucrose by *GmSuSy*. Picture from [27].

Due to low water solubility of hydrophobic phloretin (0.2 mM) DMSO was added to boost the yield of the reaction to 5 mM of nothofagin [28]. An even greater concentration of 44 mM was reached by feeding of phloretin, but high catalyst consumption and elaborate process control were required [28]. The solubility is enhanced up to 8.5 mM by 20 mM  $\beta$ -cyclodextrin (maximum solubility at 30 °C), an oligosaccharide with 7  $\alpha$ -1-4-glycosidic bonded glucopyranose units. Upon using  $\beta$ -cyclodextrin as solubility enhancer instead of DMSO the initial reaction rate  $r_{\text{nothofagin}}$  and enzyme stability of *OsCGT* and *GmSuSy* was enhanced.

## 2 Objectives

Immobilization of enzymes can reduce the costs of catalysts used in biocatalytic reaction through easy separation from the reaction mixture and possible reuse. The aim of this study was to create a protein-based affinity matrix as immobilization tool based on SAV with fused Z<sub>basic2</sub>-tag. The expression and purification of recombinant SAV in suitable amounts and the maximum loading of it to underivatized silica beads and ion exchange resin will be analysed. The coupled synthesis of nothofagin by C-glucosyltransferase from rice (*Oryza sativa*) and the regeneration of glycosyl-donor UDP-glucose by sucrose synthase from soybean (*Glycin max*) should be applied as model reaction. Therefore, both enzymes will be immobilized to the obtained affinity matrix and multiple reaction cycles with quantification of substrates and products via HPLC are intended. In the end the carrier as well as the generated protein-based affinity matrix should be regenerated and reused.

### 3 Material and methods

Unless stated otherwise, all materials were from Sigma-Aldrich in highest purity available and all operations were performed at room temperature (RT).

#### 3.1 Expression of recombinant SAV

##### 3.1.1 Cytoplasmic expression of recombinant Z<sub>basic2</sub>-SAV in *E. coli*

For the expression of SAV with N-terminal Z<sub>basic2</sub>-tag (Z<sub>basic2</sub>-SAV) BL21 (DE3)/pLysS cells containing the plasmid pT7ZbQGKlenow (description of plasmid [29]) were grown according to Humbert et al. [17] (schematic representation of gene see appendix Fig. 7-1, sequence Fig. 7-2 ). Therefore 50 mL of modified tryptone-phosphate (MTP) media (20 g L<sup>-1</sup> tryptone, 1.3 g L<sup>-1</sup> Na<sub>2</sub>HPO<sub>4</sub>, 1 g L<sup>-1</sup> KH<sub>2</sub>PO<sub>4</sub>, 8 g L<sup>-1</sup> NaCl, 15 g L<sup>-1</sup> yeast extract) supplemented with 60 µg mL<sup>-1</sup> sterile filtrated kanamycin and 34 µg mL<sup>-1</sup> sterile filtrated chloramphenicol were inoculated with 20 µL of an *E. coli* glycerol stock as precultures. The 50 mL precultures were grown in 250 mL baffled shake flasks overnight at 37 °C and 120 rpm (Pilot-Shake RC-2-TE, Adolf Kühner AG). To inoculate the 300 mL main culture in 1 L baffled shake flasks to an OD<sub>600</sub> of 0.2 the appropriate volume of preculture was mixed with 6 mL of 20 % w/v glucose solution and added to the main culture. Cultures were induced by adding sterile filtered isopropyl-β-D-thiogalactopyranoside (IPTG) to a final concentration of 0.4 mM when reaching an OD<sub>600</sub> of 1.8 to 2.2. The cultures were harvested after 3 h incubation at 37 °C and 120 rpm by centrifugation for 30 min at 5000 g and 4 °C. The pelleted cells were resuspended in dH<sub>2</sub>O (1:2) and stored at -20°C until disruption.

##### 3.1.2 Expression of Z<sub>basic2</sub>-SAV in bioreactor

The expression was also done in a 2.5 L bioreactor (Labfors 3, Infors HT) under controlled pH and pO<sub>2</sub> conditions. 2 M KOH, 1 M H<sub>3</sub>PO<sub>4</sub>, 20 % w/v glucose solution and antifoam

polypropylene glycol (PPG) were prepared and autoclaved. The pO<sub>2</sub>-sensor of bioreactor was calibrated with gasing-out method using nitrogen. 1.8 L of MTP media were autoclaved within the bioreactor and 60 µg mL<sup>-1</sup> sterile filtrated kanamycin and 34 µg mL<sup>-1</sup> sterile filtrated chloramphenicol were added afterwards. 50 mL MTP media preculture was inoculated with 20 µL of *E. coli* glycerol stock and grown in 250 mL baffled shake flasks overnight at 37 °C and 120 rpm (Pilot-Shake RC-2-TE, Adolf Kühner AG). Before inoculation of the bioreactor MTP media was pre-heated to 37 °C and stirred at 600 rpm. Bioreactor was inoculated to an OD<sub>600</sub> of 0.2 afterwards. The appropriate volume (40.7 mL) of preculture was mixed with 20 % w/v glucose solution to give a final concentration of 0.4 % glucose in the bioreactor. pH was set to 7 (controlled with 2 M KOH and 1 M H<sub>3</sub>PO<sub>4</sub>) and pO<sub>2</sub> was set to >40 %. OD<sub>600</sub> was measured every ~30 min until reaching an OD<sub>600</sub> of 1.8-2.2. Then cells were induced adding sterile filtered IPTG to a final concentration of 0.4 mM. OD<sub>600</sub> measurement was continued until harvesting after 3 h by centrifugation for 30 min at 5000 g and 4 °C. Pelleted cells were resuspended (1:2) with dH<sub>2</sub>O and frozen at -20 °C until further use.

### 3.1.3 Transformation and Expression of Z<sub>basic2</sub>-SAV in other *E. coli* strains

The expression strains *E. coli* (C41 (DE3), C41 (DE3) pLysS, BL21-Gold(DE3), C43 (DE3)) were created by transformation with SAV-pT7ZbQGKlenow plasmid and screened for higher expression levels of Z<sub>basic2</sub>-SAV. The plasmid was isolated from *E. coli* BL21-Gold(DE3) pLysS cells with GeneJET Plasmid Miniprep Kit (ThermoFisher Scientific) and digested with NcoI to digest pLys (FastDigest NcoI, ThermoFisher Scientific) and alkaline phosphatase (FastAP, ThermoFisher Scientific) according to manufacturer. 50 µL of electrocompetent cells for each strain were transferred into a precooled electroporation cuvette and 1 µL the plasmid preparation was added. After 5 min incubation on ice electroporation was done with a MicroPulser electroporator (BioRad) using the present protocol EC2. The cells were

transferred afterwards into 1 mL of prewarmed super optimal broth (20 g L<sup>-1</sup> tryptone, 5 g L<sup>-1</sup> yeast extract, 10 mM NaCl, 2.5 mM KCl, 10 mM MgCl<sub>2</sub>, 10 mM MgSO<sub>4</sub>, 20 mM glucose) and regenerated for 1 h at 37 °C and 400 rpm (thermomixer). 10 µL, 20 µL and the residual volume of the regeneration culture were streaked out on lysogeny broth agar plates (5 g L<sup>-1</sup> yeast extract, 10 g L<sup>-1</sup> tryptone, 5 g L<sup>-1</sup> NaCl, 10 g L<sup>-1</sup> agar) containing respective antibiotic (60 µg mL<sup>-1</sup> kanamycin and additionally 34 µg mL<sup>-1</sup> chloramphenicol for strains with pLysS plasmid). The plates were incubated overnight at 37 °C. 50 mL of MTP media in 250 mL baffled shake flask were inoculated with a fresh colony and incubated at 37 °C and 120 rpm (Pilot-Shake RC-2-TE, Adolf Kühner AG) overnight. Remaining procedure of expression in shake flasks was done as mentioned.

#### 3.1.4 Periplasmic expression Z<sub>basic2</sub>-SAV with the signal sequence OmpA

For periplasmic expression the gene of Z<sub>basic2</sub>-SAV was synthesized and cloned into pET-26b(+) with the signal sequence for outer membrane protein A (OmpA) of *E. coli* at the N-terminus by GenScript (pET-26b(+) *OmpA* Strep-mut). The gene for recombinant SAV (schematic representation of gene see appendix Fig. 7-3, sequence see Fig. 7-4) was inserted between the two restrictions sites for NcoI and XhoI in pET-26b(+)-vector. Additionally, a tobacco etch virus protease cleavage site (TEV) was inserted, for the cleavage of signal sequence and T7-tag after expression (schematic representation see appendix Fig. 7-3, sequence). *E. coli* expression strains were created by transformation of BL21-Gold (DE3) and BL21-Gold (DE3) pLysS electrocompetent cells, regenerated and streaked out on LB agar plates as described before (see 3.1.3). An Overview of growth media and expression conditions is shown in Tab 3.1.. In general 50 mL of LB media or terrific broth (TB) media (12 g L<sup>-1</sup> Tryptone, 24 g L<sup>-1</sup> yeast extract, 0,4 % v/v glycerol, sterile filtrated 10 x phosphate buffer 0.17 M KH<sub>2</sub>PO<sub>4</sub> and 0.72 M K<sub>2</sub>HPO<sub>4</sub>) in 250 mL baffled shake flask were inoculated with

a fresh colony of *E. coli*. and incubated overnight at 37 °C and 400 rpm (Certomat BS-1, Sartorius Stedim Biotech). Afterwards 300 mL in 1 L baffled shake flask of respective media was inoculated to an OD<sub>600</sub> of 0.2 with appropriate volume of preculture and incubated at respective temperature at 400 rpm (Certomat BS-1, Sartorius Stedim Biotech). After induction at OD<sub>600</sub> of 1.8 to 2.2 with IPTG (0.4 mM) periplasmic expression of Z<sub>basic2</sub>-SAV was done under altering incubation times and cultivation temperatures following harvest after the shown incubation time in Tab. 3-1 by centrifugation for 30 min at 5000 g and 4 °C. Pelleted cells were resuspended (1:2) with dH<sub>2</sub>O and frozen at -20 °C until disruption.

**Tab. 3-1: Expression conditions screened for periplasmic expression of Z<sub>basic2</sub>-SAV in *E. coli*.**

Strain	Media	Expression conditions
BL21-Gold (DE3)	LB	overnight at 18 °C
BL21-Gold (DE3)	LB	3 h at 37 °C
BL21-Gold (DE3)	TB	overnight at 16 °C
BL21 -Gold (DE3) pLysS	LB	overnight at 25 °C
BL21 -Gold (DE3) pLysS	LB	3 h at 37 °C

### 3.2 Protein purification of recombinant SAV

The frozen cell pellets (diluted 1:2 with dH<sub>2</sub>O before freezing) were thawed and disrupted by 3 passages through a cooled French press at 100 bar or sonication in an ice bath (Branson sonifier 250, 3 times 3 min, 1 min pause between cycles, 70 % duty cycle, output control 7). The cell debris was removed by centrifugation (14000 g, 30 min at 4 °C). After that Z<sub>basic2</sub>-SAV was purified from cell extract either with cation exchanger resin (Fractogel® EMD SO<sub>3</sub>- (M)-solution; Merck) in a 2 mL reaction vessel (see 3.2.1) or with prepacked cation exchange column with sepharose (HiTrap™ IEX SP FF, GE Healthcare) connected to an Äkta FPLC system (GE Healthcare) described in 3.2.2 .

### 3.2.1 Development of standard purification protocol of SAV with Fractogel®

For batch purification each washing, equilibration and elution cycle lasted for 15 min and incubation was performed on an end-over-end rotator at 20 rpm (Stuart rotator SB3) at RT. The supernatant was removed after spinning down the resin. 500  $\mu$ L (~57.5 mg) of resin solution (11.5 % dry matter, determined after drying at 105 °C overnight) was used and given in a 2 mL tube. The resin was prepared by washing three times with 1 mL dH<sub>2</sub>O. Afterwards the resin was equilibrated in three cycles applying 1 mL of 1 x washing buffer (50 mM CAPS, pH 11) supplemented with 500 mM NaCl (see Tab. 3-2). Cell extract was diluted 10:1 with 10x resuspension buffer (500 mM CAPS, pH 11) and filtrated through 1.2  $\mu$ m cellulose-acetate filter (Sartorius). After adding 1 mL cell lysate (total protein concentration ~80 mg/mL) the resin was washed 3 times with 1 mL 1 x washing buffer containing 500 mM NaCl. Z<sub>basic2</sub>-SAV was eluted by applying 1 x elution buffer (50 mM TRIS, pH 8.5 supplemented with 2 M NaCl) in several cycles. All fractions of the purification were collected, analyzed with SDS-PAGE and the protein concentration was determined by measuring absorbance ( $A_{280}$ , DS-11 Spectrophotometer, DeNovix). The elution fractions, which contained Z<sub>basic2</sub>-SAV, were pooled, concentrated with ultrafiltration units (Vivaspin® with 30 kDa MWCO, Sartorius) and the buffer was exchanged to 20 mM HEPES pH 7.5. The resulting concentrate was stored at 4 °C until use.

To maximize purity and yield, pH and NaCl concentration of the washing buffer (W1-W10) and resuspension buffer (R1-R5) were optimized. Therefore 1 mL resuspended cell extract was applied to 500  $\mu$ L (~57.5 mg) resin. The protein concentration of the elution fractions was measured ( $A_{280}$ ) and the purity of the elution fractions was analyzed by SDS-PAGE.

**Tab. 3-2: Screening of pH and NaCl concentration of washing buffer for the batch purification of Z<sub>basic2</sub>-SAV.**

resuspension buffer (R) <sup>*1</sup>	washing buffer (W) <sup>*2</sup>	pH	NaCl [mM]	CAPS [mM]	Tris [mM]
R1	W1	8	-	-	50
R1	W2	8	150	-	50
R1	W3	8	500	-	50
R2	W4	8.5	-	-	50
R2	W5	8.5	150	-	50
R2	W6	8.5	500	-	50
R3	W7	9.0	-	-	50
R3	W8	9.0	150	-	50
R3	W9	9.0	500	-	50
R4	W10	10	-	50	-
R4	W11	10	500	50	-
R5	W12	11	-	50	-
R5	W13	11	500	50	-

\*1 Cell extract was brought to respective pH with 10 x resuspension buffer Rx

\*2 After applying cell extract, Fractogel® was washed three times with respective washing buffer

### 3.2.2 Column purification of SAV with Äkta FPLC

All operations regarding column purification were done at RT. For the purification the thawed cell extract was diluted 1:2 with washing buffer (50 mM HEPES, pH 7) and filtrated through 1.2 µm cellulose-acetate filter (Sartorius). A prepacked sepharose column SP FF (1 mL bed dimension 7 x 25 mm or 5 mL bed dimension 16 x 25 mm, according to manufacturer) was washed with 5 column volumes (CV) of dH<sub>2</sub>O and equilibrated with 5 CVs of washing buffer (50 mM HEPES, pH 7) at constant flow rates of 1 mL min<sup>-1</sup> and 5 mL min<sup>-1</sup> for 1 mL and 5 mL columns, respectively. During loading and elution 4 mL fractions were collected using the autosampler. 10 mL prepared cell lysate (total protein concentration ~80 mg mL<sup>-1</sup>) were applied

per prepacked mL of resin. Due to higher pressure during loading of the prepared cell extract flow was reduced accordingly. Z<sub>basic2</sub>-SAV was eluted with a linear 20 CV long gradient up to 50% of elution buffer (50 mM HEPES, pH 7) containing 4 M NaCl. Elution fractions contained ~ 0.5 mg mL<sup>-1</sup> total protein. All fractions were collected, purity was analyzed by SDS-PAGE and the protein concentration was determined by measuring absorbance (A<sub>280</sub>, DS-11 Spectrophotometer, DeNovix).

### 3.3 Determination of purity using SDS-PAGE

Purity of fractions from purification was analyzed with SDS-PAGE. The samples were prepared by adding 3 µL 4x NuPAGE LDS Sample Buffer, 1.2 µL of 10x NuPAGE Reducing Agent to give 12 µL in total per sample. Samples heated for 10 min at 95 °C for the visualization of the monomeric form of Z<sub>basic2</sub>-SAV. For visualization of tetrameric form non-heated samples were applied. 10 µL of prepared sample was loaded on a protein gel (NuPAGE™ Novex™ 4-12% Bis-Tris Protein Gels) and developed at constant 200 V for 35 min with precooled MES running buffer (50 mM MES, 0.1 % w/v SDS, 50 mM Tris, 1 mM EDTA, pH 7.3). The gel was stained with 1 % Coomassie Blue staining solution (40 % v/v ethanol, 10 % v/v acetic acid, 50 % v/v dH<sub>2</sub>O) for 1 h and subsequently destained with the same solution lacking Coomassie Blue.

### 3.4 Determination of maximum protein loading of Fractogel®

Fractogel® is delivered in 20 % ethanol solution with 150 mM NaCl. The dry content was determined in triplicates with 300 µL of the carrier, which were dried for 42 h at 105 °C in an oven. For the determination of maximum loading capacity 100 µL (11.5 mg) of the carrier solution were given into a 2 mL reaction vessel. The carrier was washed with dH<sub>2</sub>O and equilibrated with washing buffer (50 mM CAPS pH 11 supplemented with 500 mM NaCl). Four times 1 mL of 2.85 mg mL<sup>-1</sup> purified Z<sub>basic2</sub>-SAV solution were applied and the amount of protein

in the supernatants was determined ( $A_{280}$ ). The carrier was washed three times with washing buffer and the protein was eluted by applying three times 1 mL washing buffer supplemented with 2 M NaCl. The loading capacity was determined according to equation 1:

$$\text{maximum } Z_{\text{basic2}}\text{SAV loading} = \frac{\sum m_{\text{prot.}} - \sum m_{\text{prot. sup}} - \sum m_{\text{prot. wash}}}{m_{\text{dry carrier}}} \quad \text{Eq. 1}$$

maximum $Z_{\text{basic2}}$ SAV loading	$[\text{mg}_{\text{protein}} \text{g}_{\text{carrier}}^{-1}]$
$\sum m_{\text{prot.}}$	total $Z_{\text{basic2}}$ -SAV offered [mg]
$\sum m_{\text{prot. sup}}$	total protein in the supernatants during loading [mg]
$\sum m_{\text{prot. wash}}$	total protein in the supernatants of the wash fractions [mg]
$m_{\text{dry carrier}}$	mass of dry carrier used [g]

### 3.5 Determination of maximum protein loading of underivatized silica beads

To determine the maximum protein loading of underivatized silica beads (Trisoperl, VitraBio GmbH) purified  $Z_{\text{basic2}}$ -SAV was immobilized on 51.8 mg of carrier. The beads were rinsed with  $\text{dH}_2\text{O}$  followed by three cycles of equilibration with 1 mL of washing buffer (20 mM HEPES pH 7.5) and incubation for 10 min on end-over-end rotator (20 rpm). Afterwards a total of 5.44 mg  $Z_{\text{basic2}}$ -SAV were applied to the carrier and the mixture was incubated on an end-over-end rotator (20 rpm) in eight consecutive cycles. After the settlement of the beads the supernatant of each cycle was analyzed for unbound  $Z_{\text{basic2}}$ -SAV left in solution. After that the carrier was washed four times with washing buffer containing 500 mM of NaCl. Elution of  $Z_{\text{basic2}}$ -SAV and calculation were done according to the procedure for Fractogel®.

### 3.6 Immobilization of *OsCGT* and *GmSuSy* on SAV affinity matrix

For the enzymatic reaction with immobilized enzyme 99.6 mg of underivatized silica beads were rinsed with water and incubated with purified Z<sub>basic2</sub>-SAV overnight on an end-over-end rotator at 20 rpm for binding (loading 44 mg<sub>protein</sub> g<sub>carrier</sub><sup>-1</sup> Z<sub>basic2</sub>-SAV). After that the carrier was equilibrated with washing buffer (50 mM HEPES pH 7.5) before adding of 200 µg purified *GmSuSy* (GenBank: AF030231) and purified *OsCGT* (GenBank: FM179712) followed by 15 min incubation on end over end rotator. Unbound enzyme was washed away with washing buffer and 15 min incubation on end over end rotator. The expression of both enzymes is described elsewhere [27].

Cyclodextrin was dissolved first to a final concentration of 15 mM in dH<sub>2</sub>O. After that 2 mM phloretin (Carbosynth), 100 mM sucrose, 0.25 mM UDP disodium salt (Carbosynth), 13 mM MgCl<sub>2</sub>, 50 mM KCl, 0.13 % (w/v) BSA and 50 mM HEPES were added and the pH was set to 7.5 resulting in the final reaction solution. Synthesis was started by the addition of 1 mL of the reaction solution to the prepared carrier. After 15 min incubation at 20 rpm on end over end rotator the carrier was separated from the reaction solution by a short centrifugation. 25 µL sample were stopped immediately by adding of 25 µL ACN. An additional sample was taken from the remaining solution (without solid carrier) after 15 min of incubation on the end-over-end rotator to check for residual enzymatic activity in the reaction solution. UDP-glucose, UDP, nothofagin and phloretin were quantified in a single run with an extended reversed-phase ion-pairing HPLC method described elsewhere [30]. The reaction rate  $r_{nothofagin}$  was calculated according equation 2:

$$r_{nothofagin} [\mu M \text{ min}^{-1}] = \frac{c_{nothofagin} [\mu M]}{t_{incubation} [\text{min}]} \quad \text{Eq. 2}$$

$r_{nothofagin}$  coupled syntheses rate [ $\mu M \text{ min}^{-1}$ ]

$c_{nothofagin}$  concentration of nothofagin [ $\mu M$ ]

$t_{incubation}$  reaction time [min]

After completing enzymatic reactions, the carrier was prepared for further experiments with regeneration buffer.

### 3.7 Regeneration of SAV affinity matrix

The affinity matrix was regenerated after use in enzymatic reactions by applying 1 mL of strep-regeneration buffer (100 mM TRIS, 150 mM NaCl, 1 mM EDTA, 10 mM HABA (2-(4-Hydroxyphenylazo)benzoic acid, pH 8). After that the carrier was washed with washing buffer (regeneration buffer lacking HABA) until the red color of SAV-HABA complex disappeared.

## 4 Results and Discussion

### 4.1 Cytoplasmic expression of recombinant SAV

The expression of the ligand in suitable amounts is mandatory for effective and cost-efficient generation of the affinity matrix. Therefore, an optimized expression protocol for recombinant SAV as well as the expression in different *E. coli* strains were tested. All strains were cultivated on MTP media in shaking flasks or bioreactor. In shake flasks the highest protein concentration of 4.25 mg L<sub>media</sub><sup>-1</sup> was reached with *E. coli* BL21-Gold (DE3) pLysS. *E. coli* C41 (DE3) derived from BL21-Gold (DE3) and C43 (DE3) derived from C41 (DE3), which contained uncharacterized mutations for resistance against toxic proteins did not show higher expression levels of Z<sub>basic2</sub>-SAV (see Tab. 4-1). When BL21-Gold (DE3) pLysS was cultivated in a controlled bioreactor the concentration was increased up to 6.91 mg L<sub>media</sub><sup>-1</sup>.

**Tab. 4-1: Protein expression yield of Z<sub>basic2</sub>-SAV in different *E. coli* strains.**

<i>E. coli</i> expression strain	cultivation	Expression yield of Z <sub>basic2</sub> -SAV [mg L <sub>media</sub> <sup>-1</sup> ]
BL21-Gold (DE3) pLysS	Shaking flask	4.25
BL21-Gold (DE3) pLysS	bioreactor	6.91
C41 DE3	Shaking flask	2.22
C41 DE3 pLysS	Shaking flask	1.78
C43 DE3	Shaking flask	0.62

The routinely reached 100-120 mg L<sub>media</sub><sup>-1</sup> of protein reported by Humbert et al. with a different SAV construct were not reached [17]. For simplification of the expression protocol and development of a one-step purification/immobilization procedure the de- and renaturation step was skipped. This was probably a crucial factor that lead to lower yield. The tendency of *E. coli* to express SAV in inclusion bodies and the need for protein refolding to maximize yield of

functional protein were described in different expression protocols [19, 31, 32]. However, it has to be noted that existing SAV refolding protocols would likely need significant adaption for refolding in presence of the large  $Z_{\text{basic2}}$ -tag. 17 mg of remaining insoluble pellet (after disruption and separation from dissolved fraction) was resuspended in 70  $\mu\text{L}$   $\text{dH}_2\text{O}$ , further diluted 1:5 with  $\text{dH}_2\text{O}$  and analyzed by SDS-PAGE. A thin band was seen at 27 kDa in the insoluble pellet fraction (lane 3) characteristic for  $Z_{\text{basic2}}$ -SAV giving evidence for only small remaining amounts in the insoluble pellet fraction.

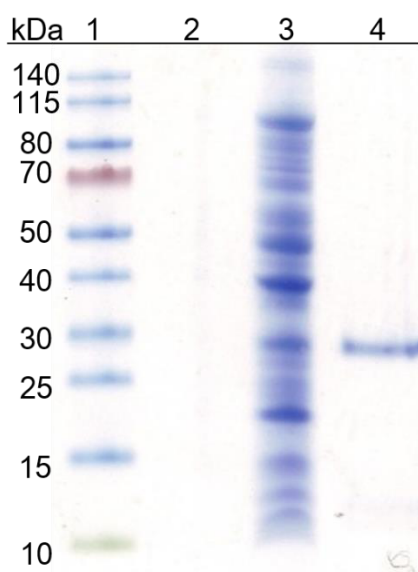


**Fig. 4-1 SDS-PAGE analysis of undissolved pellet after separation from dissolved cell extract.** Lane 1: molecular weight marker; lane 2: undiluted undissolved pellet (overloaded); lane 3: 1:5 undissolved pellet; lane 4: purified  $Z_{\text{basic2}}$ -SAV.

The growth of *E. coli* BL21-Gold (DE3) pLysS was slowing down relatively fast and the exponential growth ended around 1 h 30 min post induction (see appendix Fig. 7-5). Humber et al. [17] noted that the amount of SAV expressed per cell was very similar in different screened medias. Therefore, the optimal growth of the cells appears as a critical factor in expression. This could be the cause for the slightly increase in protein concentration when using the pH and  $\text{pO}_2$  controlled bioreactor. Further analysis of the possibly formed inclusion bodies as well as a renaturing strategy should be developed to increase the yield of  $Z_{\text{basic2}}$ -SAV expression.

## 4.2 Periplasmic expression of Z<sub>basic2</sub>-SAV

A strategy that should prevent the toxicity of Z<sub>basic2</sub>-SAV to *E. coli* is the guided translocation of the protein into periplasmic space [21]. The signal sequence for *OmpA* was introduced and the resulting plasmid pET-26b(+) *OmpA* Strep-mut was transformed into the two *E. coli* strains BL21-Gold (DE3) and BL21-Gold (DE3)/pLysS. Two different media (LB and TB), induction time (3 h to overnight) and temperature (16 °C; 18 °C; 25 °C; 37 °C) were screened for optimal expression. SDS-PAGE analyses revealed a strong band at 27 kDa in the cell extract of BL21-Gold (DE3) after growing the cells overnight at 18 °C in LB media (see Fig. 4-2 lane 1, b). Due to the elevated heat stability of SAV the tetrameric structure stays intact when the heat incubation is omitted in the preparation of SDS-PAGE samples [18]. The tetrameric structure was confirmed in the cell extract by applying a non-heated sample (lane c). Unfortunately, after the standard purification with Fractogel® (see 4.3) the elution fractions did not show a band characteristic for Z<sub>basic2</sub>-SAV. The protein was not able to bind, which was confirmed by nearly the same intensity of band in cell extract and flow through.

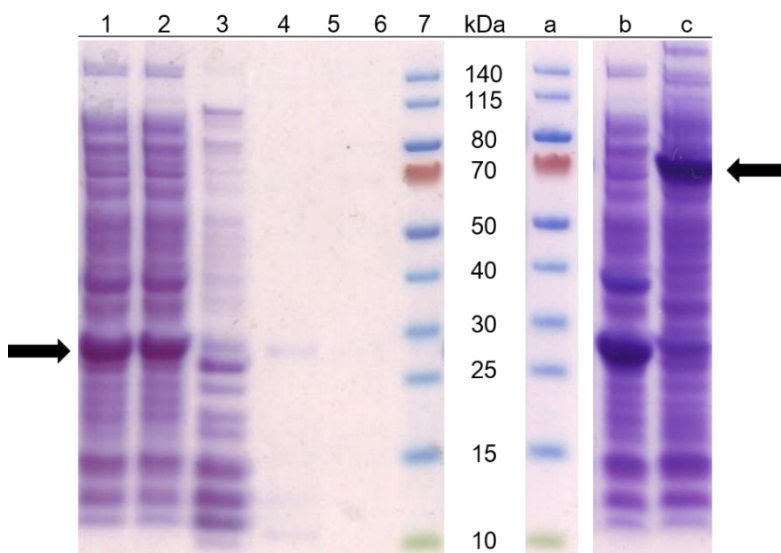


**Fig. 4-2: SDS-PAGE analysis of purification fractions containing Z<sub>basic2</sub>\_SAV (indicated by arrows) expressed in the periplasm of *E. coli*/BL21-Gold (DE3). Lane 1: cell extract; lane 2: flow through; lane 3: wash; lane 4, 5, 6: elution fraction 1, 2, 3; lane 7, a: molecular weight marker; lane b: cell extract (sample heated for 10 min at 95 °C); lane c: cell extract (sample not heated).**

The cell extract was also digested with TEV protease to cleave T7 tag and *OmpA* signal sequence, which could have interfered with the binding of  $Z_{\text{basic2-SAV}}$  to the resin. Elution fraction showed a thin band corresponding to  $Z_{\text{basic2-SAV}}$ , but the concentration was again too low for protein quantification. When growing BL21-Gold (DE3) overnight in TB media at 16 °C to enrich final cell density, analyses of cell extract revealed a much lower expression of  $Z_{\text{basic2-SAV}}$  compared to expression in LB media. The cell extract, the cell extract digested with TEV protease and cell extract from cytoplasmic expression (as standard) were applied to prepacked sepharose columns connected to an Äkta system in individual runs for comparison, therefore. Elution fractions of cytoplasmic expressed  $Z_{\text{basic2-SAV}}$  showed a major band around 73 kDa even without concentrating the sample. For the periplasmic expression, only the strongly concentrated and pooled elution fractions with subsequent TEV digestion showed a band at around 65 kDa. The cleaved monomeric *OmpA* $Z_{\text{basic2-SAV}}$  has a molecular weight of 22.497 kDa (89.991 kDa tetramer) in contrast to  $Z_{\text{basic2-SAV}}$  having 26.136 kDa (104.548 kDa tetramer). The lower molecular weight was caused by missing T7-tag and linker amino acids which explains the detected small size difference in SDS-PAGE (molecular weight was calculated based on the sequence with ExPASy-Compute pI/Mw tool [33]).

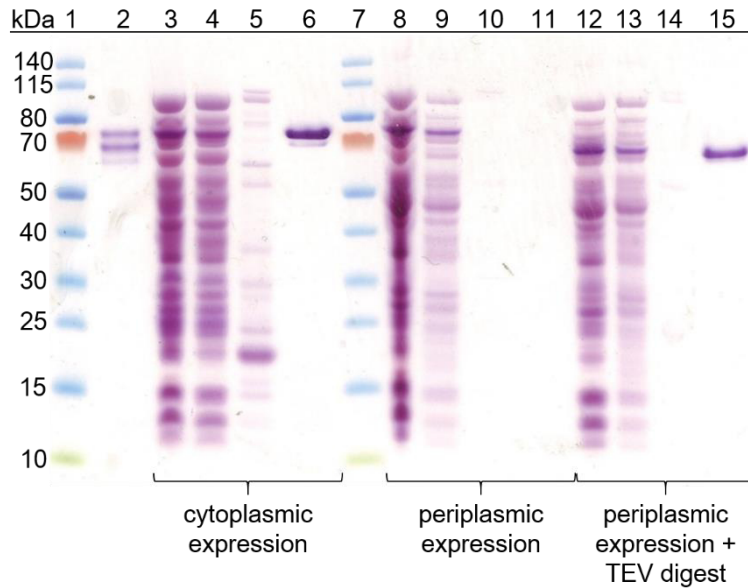


**Fig. 4-3: SDS-PAGE analysis of purification fractions containing  $Z_{\text{basic2\_SAV}}$  from cytoplasmic expression in *E. coli*/BL21-Gold (DE3) pLysS and periplasmic expression in *E. coli*/BL21-Gold (DE3) in TB media at 16 °C overnight.** Lane 1, 7: molecular weight standard; lane 2: purified standard of  $Z_{\text{basic2\_SAV}}$ ; lane 3, 8, 12: cell extract; lane 4, 9, 13: flow through; lane 5, 10, 14: wash fraction; lane 6, 11, 15: elution fraction. The sample of lane 15 was concentrated with ultrafiltration units.

Overall, the periplasmic expression of  $Z_{\text{basic2\_SAV}}$  caused a decreased productivity of purified protein although the expression level revealed in electrophoretic analyses appears promising. Therefore, it seems that toxicity of  $Z_{\text{basic2\_SAV}}$  caused by the biotin depletion is overcome by the guided translocation to the periplasm using the signal sequence *OmpA*. The occurring problems during purification could be caused by e.g. unsuccessful cleavage of the signal sequence. This could probably result in folding issues of  $Z_{\text{basic2\_tag}}$  preventing the binding to the purification resin. This is underlined when TEV protease is applied subsequently to the cell extract causing a more successful purification. The final obtained yield of soluble  $Z_{\text{basic2\_SAV}}$  from periplasmic expression appeared to be too low for further use.

### 4.3 Development of a purification procedure of Z<sub>basic2</sub>-SAV

For the characterization of immobilization of Z<sub>basic2</sub>-SAV to different carriers, the demand of protein purity is high to avoid interfering effects (protein-protein interactions, interactions of the carrier with other proteins than the aimed ligand). An optimized procedure to purify Z<sub>basic2</sub>-SAV in > 90% purity from crude cell extract of *E. coli* was developed. This was accomplished in a series of purification experiments using strong ion exchanger resin Fractogel®. The influence of increasing pH and salt concentration of the washing buffer was studied. Before loading, the cell extract was brought to pH of the respective washing buffer. Almost independent from pH the increasing NaCl concentration prevented the unspecific binding of other proteins than Z<sub>basic2</sub>-SAV. Already at pH 8 and 500 mM NaCl a relatively high purity of Z<sub>basic2</sub>-SAV was reached after the elution with buffer containing 2 M NaCl. Increasing pH led to lower unspecific binding of proteins even though to a much lower extent. Upon applying buffer with a pH of 11 supplemented with 500 mM NaCl the highest purity was obtained. The amount of Z<sub>basic2</sub>-SAV appeared to decrease between pH 10 (0.44 mg mL<sup>-1</sup>) and pH 11 (0.37 mg mL<sup>-1</sup>) by ~16 %, while purity was just slightly increased at pH 11. Nevertheless, washing buffer with a pH of 11 was chosen for the standard purification protocol to obtain the highest purity of Z<sub>basic2</sub>-SAV.

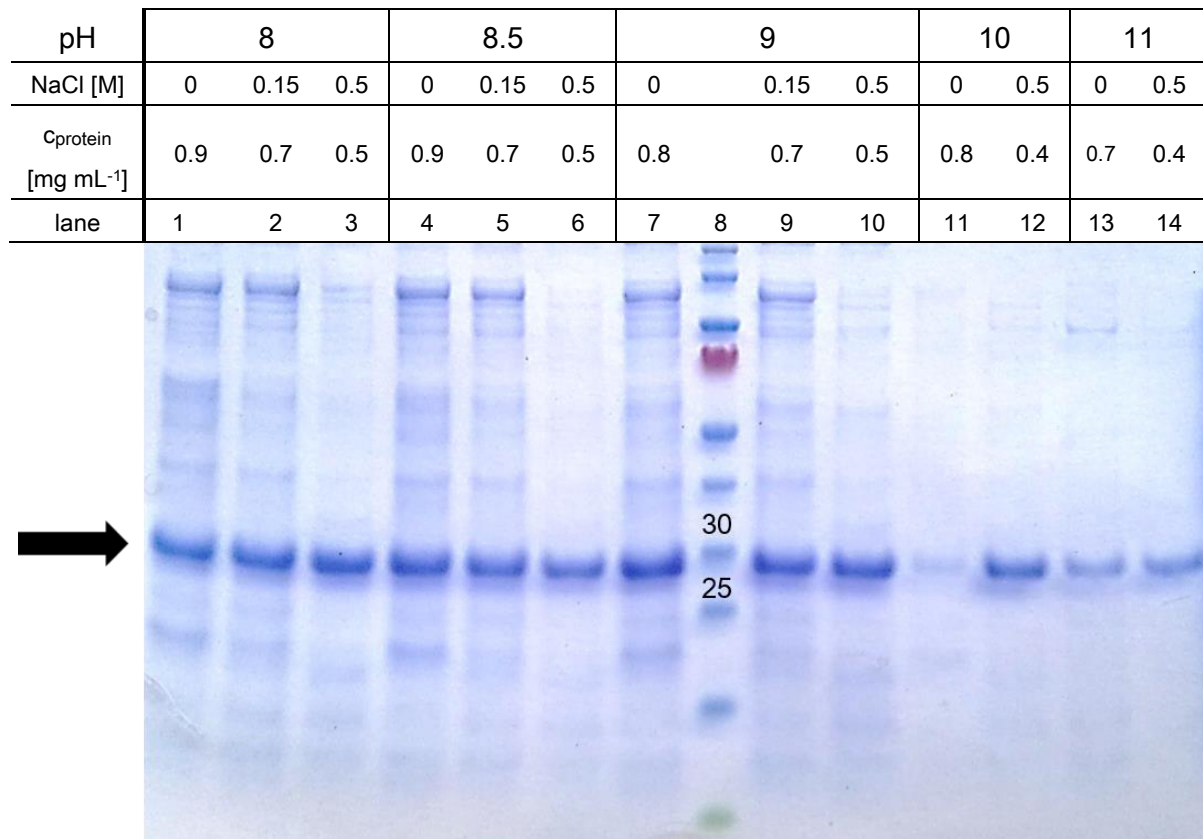


**Fig. 4-4: Optimization of washing buffer for purification of Z<sub>basic2</sub>-STV using the IEX resin Fractogel®. Analysis of elution fractions is shown.** The pH and NaCl concentration of the washing buffer were altered as indicated in the table. Cell extract of *E. coli* was brought to pH with the respective 10x resuspension buffer. Lane 1-7 and 9-14: elution fraction 1, lane 8: molecular weight marker, kDa.

These harsh conditions allowed selective binding of Z<sub>basic2</sub>\_SAV to Fractogel®. Gräslund et. al reported that purified Z<sub>basic2</sub>-peptide is binding at both pH 10 and 11, but the eluted amount of protein is reduced drastically at pH 11 [15]. This behavior is consistent with the reported pI of the Z<sub>basic2</sub>-tag (10.5) [13]. In this work hardly any reduction of protein recovery was observed by increasing the pH of the washing solution from 10 to 11. This can be explained by the higher (calculated) pI of the herein used Z<sub>basic2</sub>-tag amino acid sequence (11.40 calculated by ExPASy-Compute pI/Mw tool) [33].

## 4.4 Characterization of Z<sub>basic2</sub>-SAV affinity matrix

### 4.4.1 Maximum Z<sub>basic2</sub>-SAV loading capacity of different carriers

An essential parameter for the immobilization of proteins is the maximum protein loading per gram of carrier. The value is critical for the applicability of the immobilized catalyst for the respective operation. Therefore, the maximum loading of Z<sub>basic2</sub>\_SAV onto Fractogel® and underivatized silica beads was analyzed. Purified fractions of Z<sub>basic2</sub>\_SAV were applied in a series of loading steps. Fractogel® (291.5 mg<sub>protein</sub> g<sub>dry carrier</sub><sup>-1</sup>) showed an around six times higher maximum loading capacity than silica beads (54.3 mg<sub>protein</sub> g<sub>dry carrier</sub><sup>-1</sup>). These values correspond to theoretically available biotin binding sites of 11.2 nmol g<sub>dry carrier</sub><sup>-1</sup> and 2.1 nmol g<sub>dry carrier</sub><sup>-1</sup>, respectively. Fractogel® is optimized for purification and immobilization of proteins exhibiting a “tentacle” structure whereas the silica beads are underivatized and having a porous structure. This difference in composition could probably cause the lower maximum loading of the silica beads.

**Tab. 4-2: Determined maximum protein loading of Z<sub>basic2</sub>\_SAV of Fractogel® and underivatized silica beads.** The maximum Z<sub>basic2</sub>\_SAV loading was determined from total applied protein and protein amount in wash and supernatant fractions.

carrier	maximum Z <sub>basic2</sub> _SAV loading		theoretical biotin binding sites*1 [nmol g <sub>dry carrier</sub> <sup>-1</sup> ]
	[mg <sub>protein</sub> g <sub>dry carrier</sub> <sup>-1</sup> ]	[nmol <sub>protein</sub> g <sub>dry carrier</sub> <sup>-1</sup> ]	
Fractogel®	291.5	2.8	11.2
underivatized silica beads	54.3	0.5	2.1

\*1 Theoretical biotin binding sites are calculated using molecular weight of the monomer of Z<sub>basic2</sub>\_SAV determined by sequence of 26,137 g/mol and the assumption that all four binding sites of the tetramer are available.

In a multistep loading experiment Wiesbauer et al. [6] immobilized an oxidase from *Trigonopsis variabilis* and phosphorylase from *Leuconostoc mesenteroides* both containing Z<sub>basic</sub> binding domain to Fractogel®. Around ~ 250 mg<sub>protein</sub> g<sub>dry carrier</sub><sup>-1</sup> in four immobilization steps and around

~ 350  $\text{mg}_{\text{protein}} \text{g}_{\text{dry carrier}}^{-1}$  in three immobilization steps were reached, respectively. The enzymatic activity was reported as almost linear to the offered protein amount and the maximum loading capacity was not reached in the experiment. The maximum loading reached here is therefore in the same order of magnitude for Fractogel®. Wu et al. immobilized a recombinant SAV via non-covalent interaction of a dextran binding domain with dextran-based matrix (Sephadex®-100) [11]. They reported that 1 mL of a settled bed of the affinity matrix exhibits 20 nM available binding sites and can bind  $485 \pm 3 \mu\text{g}$  of biotinylated BSA.

#### 4.4.2 Z<sub>basic</sub>-SAV immobilized on underivatized silica beads

For the determination of loading capacity of the silica beads small portions of protein were applied to study the binding behavior in detail. 0.5 mg total protein in four loading steps followed by three loading steps with 0.8 mg total protein were applied. The course of the immobilized protein was almost linear until no more protein was bound to the carrier (see Fig. 4-5 step 8). The carrier was only washed with buffer after completing all eight loading steps. Unbound protein was only washed off during the following washing steps. Therefore, the maximum loaded protein and the immobilization yield (protein applied/maximum loading capacity) appears to exceed after loading step eight the maximum loading capacity of  $54.3 \text{ mg}_{\text{protein}} \text{g}_{\text{dry carrier}}^{-1}$  (100 % immobilization yield).

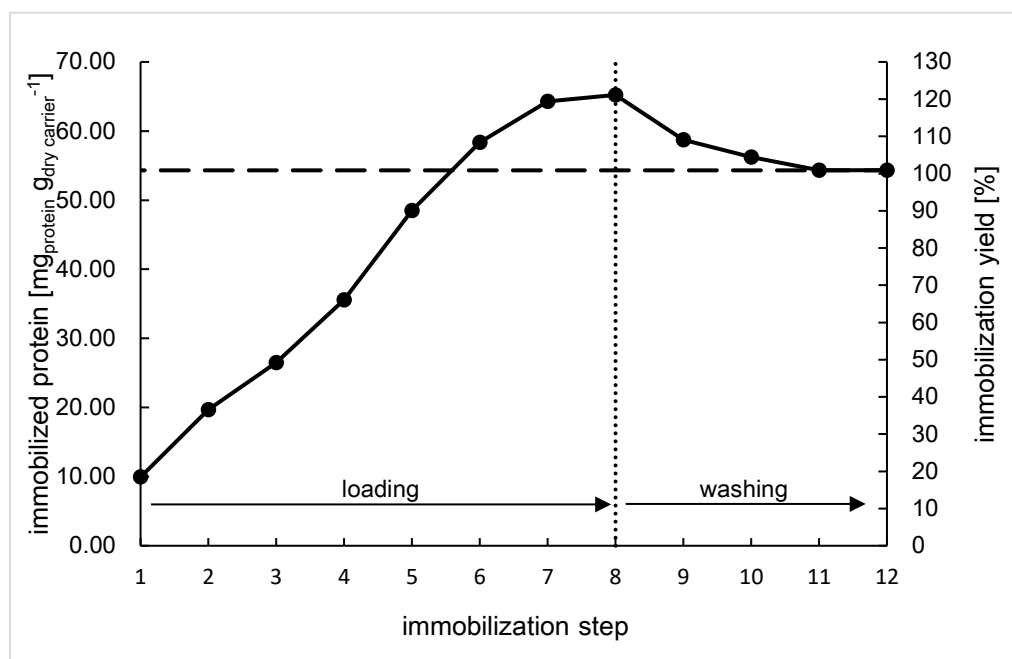


**Fig. 4-5: Determination of maximum loading of  $Z_{\text{basic}}$ -SAV on underivatized silica beads.** dotted line: end of addition of subsequently purified  $Z_{\text{basic2}}$ -SAV, dashed line: maximum loading achieved.

#### 4.4.3 Elution of protein and protein recovery

The protein was eluted from the glass beads afterwards with 50 mM Tris buffer pH 8.5 containing 2 M NaCl. In total only 0.77 mg of the immobilized 2.81 mg were eluted which equals 27 %. Elution from Fractogel® was much more effective under the same conditions, resulting 87 % of protein recovery. The effect of pH and NaCl concentration for the elution of  $Z_{\text{basic2}}$ -*Tv*DAO (D-amino acid oxidase from *Trigonopsis variabilis*) was studied by Bolivar [13]. It was mentioned, that only at high salt concentration of up to 5 M NaCl protein was eluted effectively from the same glass beads. The addition of 0.5 % Tween 20 allowed for the recovery of enzyme activity up to 100 % (pH 8; 5 M NaCl; 0.5 % Tween 20). An explanation was based on substantial hydrophobic interactions of the enzyme with the support additional to the electrostatic interactions. These interactions are probably occurring between  $Z_{\text{basic2}}$ -SAV and the silica surface as well, leading to the low elution when applying elution buffer containing only 2 M NaCl. The tetrameric form of SAV containing four  $Z_{\text{basic2}}$ -tags could probably include multiunit interactions with the silica surface, which even intensifies the binding and impedes

the regeneration of the carrier. For the complete regeneration of the underivatized silica beads higher salt concentrations and addition of Tween could improve the elution of protein.

#### 4.4.4 Regeneration of the $Z_{\text{basic2}}$ -SAV-silica beads affinity matrix

Not only the regeneration of the silica beads itself would expand the applicability of the affinity matrix also regeneration of the silica beads with bound  $Z_{\text{basic2}}$ -SAV would. Therefore, the protocol for the regeneration of commercial *Strep-Tactin*<sup>®</sup> resin was applied after the immobilization of the strep-tagged enzymes. An intense color change from yellow to red was observed implying the high availability of the biotin binding sites of the immobilized  $Z_{\text{basic2}}$ -SAV.



(A) (B)

**Fig. 4-6: Color change of  $Z_{\text{basic2}}$ -SAV-silica beads after applying regeneration buffer (HABA) for *Strep-Tactin*<sup>®</sup>.** (A): applying regeneration buffer to underivatized silica beads without immobilized  $Z_{\text{basic2}}$ -SAV, (B): applying regeneration buffer to underivatized silica beads with  $Z_{\text{basic2}}$ -SAV immobilized.

The regeneration protocol includes 2-(4-hydroxyphenylazo)benzoic acid (HABA), an organic dye that binds with lower affinity ( $K_a = 10^{-4}$  M in contrast to  $4 \times 10^{-14}$  M for biotin) to the binding pocket of SAV [34]. It replaces desthiobiotin, which is used for the elution of strep-tagged proteins during purification of enzymes with *Strep-Tactin*<sup>®</sup> resin. The complexation of HABA during binding leads to a visual color change from yellow to red [35]. The carrier with HABA

was rinsed with washing buffer afterwards. The procedure was successfully applied for the regeneration of the  $Z_{\text{basic2-SAV}}$ -beads.

## 4.5 Application of affinity matrix for immobilization and enzyme catalysis

To demonstrate one possible application of the  $Z_{\text{basic2-SAV}}$ -silica beads for immobilization a well characterized model reaction including two strep-tagged enzymes was conducted. The regenerated affinity matrix was applied for the immobilization of the two enzymes *OsCGT* and *GmSuSy* involved in the synthesis of nothofagin with included UDP-glucose regeneration (see Figure 1.3). To additionally prove the possibility of multiple use of the produced catalyst eight consecutive reactions were done and reaction products were quantified for each cycle.

### 4.5.1 Enzymatic catalysis with immobilized enzyme

99.6 mg of silica beads were loaded with  $44 \text{ mg}_{\text{protein}} \text{ g}_{\text{carrier}}^{-1} Z_{\text{basic2-SAV}}$  and 200  $\mu\text{g}$  of both enzymes were applied afterwards. The reaction was started by adding a reaction mix containing 2 mM phloretin, 100 mM sucrose and 0.25 mM UDP in consecutive repetitions. Conversion of phloretin and UDP was measured after 15 min and the carrier was separated from reaction solution. The remaining solution was again measured after 15 min to prove for residual enzyme activity.

First conversion reaction showed that 51 % given phloretin was glycosylated to nothofagin with a reaction rate  $r_{\text{nothofagin}}$  of  $67 \mu\text{M min}^{-1}$ . The conversion is decreasing to 17 % with a  $r_{\text{nothofagin}}$  of  $23 \mu\text{M min}^{-1}$  measured in seventh reaction. In total the conversion catalyzed by *OsCGT* decreased to around 30 % of the initial reaction rate. The recycling of UDP-glucose by *GmSuSy* did not appear to be the limiting factor, because at the end of the first reaction 30  $\mu\text{M}$  UDP-glucose are left in the solution and the concentration increased to 90  $\mu\text{M}$  in the eighth

reaction. The applied concentration of 0.25 mM UDP was decreasing which also implies less synthesis of nothofagin together with higher production of UDP-glucose.

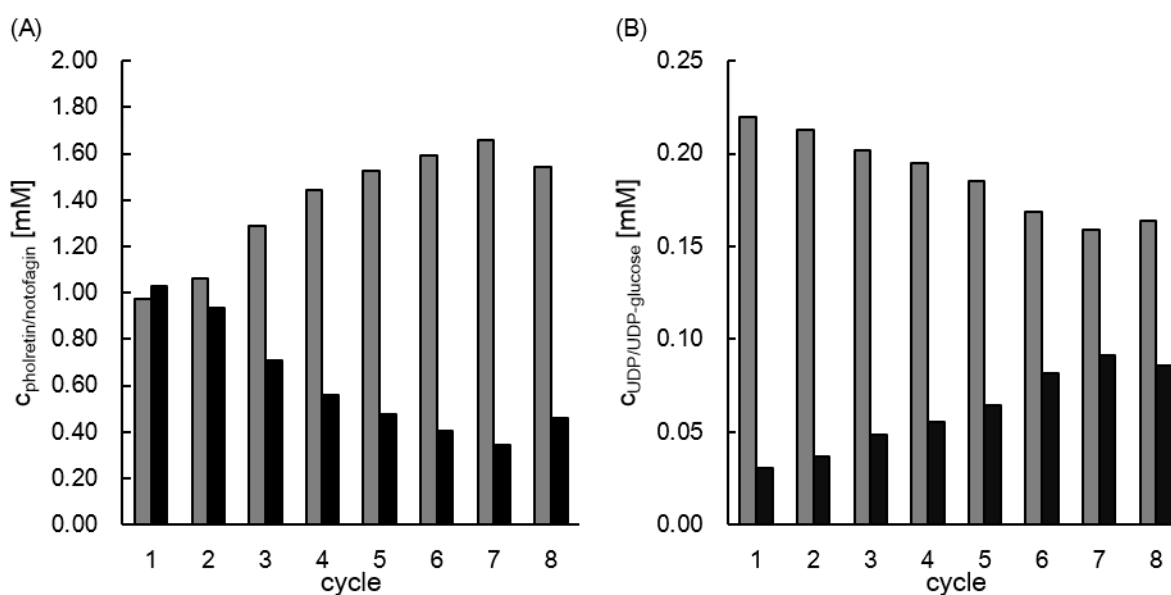


**Fig. 4-7: Multiple synthesis cycles of nothofagin with affinity immobilized *OsCGT* and *GmSuSy* ( $2 \mu\text{g}_{\text{protein}} \text{mg}_{\text{carrier}}^{-1}$  loading) on  $Z_{\text{basic2-SAV}}$ -silica beads ( $44 \text{ mg}_{\text{protein}} \text{g}_{\text{carrier}}$  loading).** Reaction mix contains 2 mM phloretin, 0.25 mM UDP and 100 mM sucrose and was incubated 15 min (RT, 20 rpm). (A)  $C_{\text{phloretin}}$  (grey bars) and  $C_{\text{nothofagin}}$  (black bars) over eight cycles using the same catalyst. (B)  $C_{\text{UDP}}$  (grey bars) and  $C_{\text{UDP-glucose}}$  (black bars).

#### 4.5.2 Analysis of reaction solutions fractions

Fractions of the enzyme immobilization process and reaction solution after incubation were analyzed with SDS-PAGE for protein content. After applying the mixed enzyme solution to the  $Z_{\text{basic2-SAV}}$ -silica beads the supernatant fractions showed clear bands for both *GmSuSy* (94.101 kDa) and *OsCGT* (51.294 kDa). The total protein amount on the gel appears greater for *GmSuSy* than for *OsCGT*, which could indicate that less *GmSuSy* was bound to the affinity matrix. During the reaction thin bands of both proteins were identified until cycle four with decreasing amounts from cycle to cycle. SDS-PAGE analysis of the different fractions did not show bands in size of  $Z_{\text{basic2-SAV}}$  implying a high stability of the binding to silica beads in the respective reaction environment.

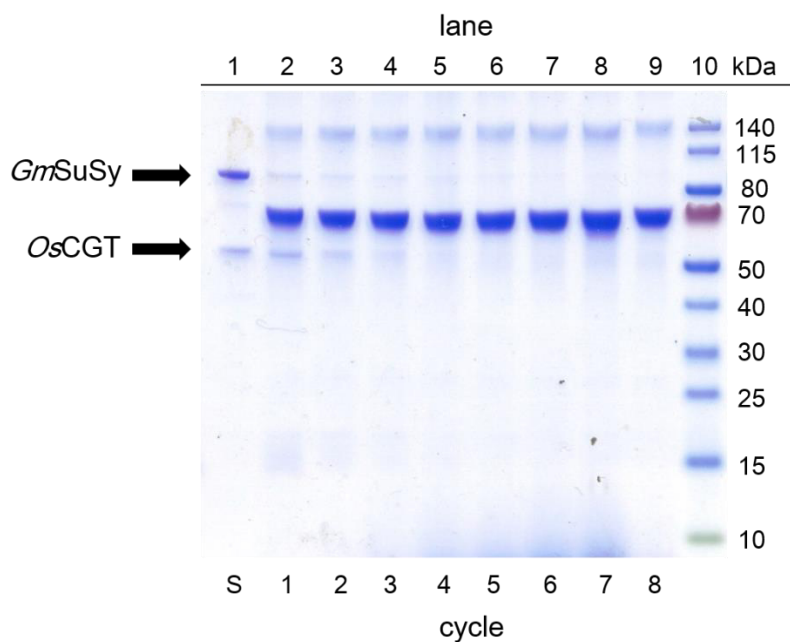


**Fig. 4-8: SDS-PAGE analysis of fractions of each cycle of the synthesis of nothofagin with immobilized *OsCGT* (51.294 kDa) and *GmSuSy* (94.101 kDa) on  $Z_{\text{basic}2}$ -SAV-silica beads.** The strong band at 70 kDa was BSA. Lane 1: supernatant fraction after immobilization; lane 2-9: reaction solution from cycle 1 to 8; 10: molecular weight marker.

#### 4.5.3 Remaining enzyme activity and recovery

The reaction solution was separated from the carrier and analyzed again after 15 min for residual enzyme activity. The conversion of phloretin to nothofagin was still present at rates between 8 % (first cycle) and 1 % (fifth cycle) of originally applied enzyme. The decrease of enzyme activity of the silica beads was compared to the remaining activity in solution. Besides the first cycle (163 %) and the last cycle (- 51 %), the lost enzyme activity of the carrier was not totally recovered in the solution without carrier. These finding implies that the enzymes are inactivated on the carrier or upon release from the carrier.

**Tab. 4-3: Analysis of reaction solution after separating the catalyst and additional incubation for 15 min.**

$r_{\text{nothofagin}}$  coupled syntheses rate.

Cycle	phloretin conversion [%]	$r_{\text{nothofagin}}$ in solution [ $\mu\text{mol min}^{-1}$ ]	loss of catalyst activity $r_{\text{nothofagin}}$ [ $\mu\text{mol min}^{-1}$ ]	recovery [%]
1	8	10	6	163
2	3	4	15	26
3	4	5	10	53

Cycle	phloretin conversion [%]	$r_{\text{nothofagin}}$ in solution [ $\mu\text{mol min}^{-1}$ ]	loss of catalyst activity $r_{\text{nothofagin}}$ [ $\mu\text{mol min}^{-1}$ ]	recovery [%]
4	2	3	6	47
5	1	1	5	32
6	2	3	4	62
7	3	4	-8	-51

Overall, both enzymes were bound to the carrier via the *strep-tag* II interaction with the affinity matrix ( $Z_{\text{basic2}}$ -SAV-silica beads). The immobilization yield (offered amount of enzyme in comparison with actual immobilized amount) appears to be lower for *GmSuSy* than for *OsCGT* (see Fig. 4-8). Both enzymes were leaking from the carrier and the reaction rate  $r_{\text{nothofagin}}$  was decreasing from cycle to cycle to about 30 % from initial rate. Residual activity is found in the solution after separation from the carrier in less amount in comparison to the lost activity of the carrier. Due to significant loss in activity and the rather low immobilization yield considerations increasing the binding strength of *strep-tag* II and  $Z_{\text{basic2}}$ -SAV in the reaction environment have to be made.

#### 4.5.4 Binding strength of *strep-tag* II and $Z_{\text{basic2}}$ -SAV

The tetrameric structure of *GmSuSy* could lead to the assumption that more than one *strep-tag* II interacts with the affinity matrix thus strengthen the binding. In contrast Skerra et al. [21] reported that they do not assume the simultaneously interaction of both tags for an dimeric alkaline phosphatase. So *GmSuSy* and *OsCGT* should probably bind with only one affinity tag to binding site of SAV. The binding affinity of SAV itself can be negatively affected by the immobilization of it to a solid surface. To prevent this, enough space between the biotin binding sites and the surface for the accessibility of ligands has to be created. Reznik et al. showed that with a small C-terminal fused six-residue sequence the covalent attachment of a SAV mutant exhibit comparable biotin-binding characteristics as in solution [36]. The  $Z_{\text{basic2}}$ -tag

---

consists of a 58 amino acid chain arranged in a three-helix bundle. It could even be too long and might sterically hinder proteins from the attachment. If the linker used in this study is appropriate to keep all binding sites available must be found out. The binding characteristics must be evaluated in solution in comparison to the immobilized Z<sub>basic2</sub>-SAV on the surface. A possible appropriate assay for the comparison of available binding site is the determination of bindings sites of SAV with biotin-4-fluorescein (B4F) [37, 38]. A B4F stock solution with known concentration is titrated to a sample of SAV. The assay relies on the strong fluorescence quenching of B4F after binding to SAV. The assay could be applied for accurate measurement of binding sites in solution and possibly also after the immobilization of Z<sub>basic2</sub>-SAV.

## 5 Conclusion and Outlook

The creation of a protein-based affinity matrix for immobilization based on  $Z_{\text{basic2-SAV}}$  was studied in this thesis. The expression of suitable amounts of soluble recombinant  $Z_{\text{basic2-SAV}}$  remains challenging due to the toxicity to *E. coli* and possible formation of inclusion bodies. The highest yield of soluble  $Z_{\text{basic2-SAV}}$  was  $6.91 \text{ mg}_{\text{protein}} \text{ L}_{\text{media}}^{-1}$  for BL21-Gold (DE3) pLysS in a pH and  $pO_2$  controlled 2-L fermenter. The yield in shaking flasks was  $4.25 \text{ mg}_{\text{protein}} \text{ L}_{\text{media}}^{-1}$  for the same strain. Other strains like *E. coli* C41(DE3) and C43(DE3) which are specially designed for recombinant expression of toxic proteins showed lower yields of  $2.22 \text{ mg}_{\text{protein}} \text{ L}_{\text{media}}^{-1}$  and  $0.62 \text{ mg}_{\text{protein}} \text{ L}_{\text{media}}^{-1}$ , respectively. The translocation of  $Z_{\text{basic2-SAV}}$  to the periplasmic space by fusing the signal sequence for outer membrane protein A (*OmpA*) to overcome the toxicity was applied therefore. The cell extract of BL21-Gold (DE3) showed a prominent band of  $Z_{\text{basic2-SAV}}$  after expression in LB media overnight at 18 °C. Unfortunately, purification of the protein yielded only very small quantities, which were even lower than from cytoplasmic expression.

The purity of the  $Z_{\text{basic2-SAV}}$  elution fraction was > 90 % (based on SDS-PAGE analysis) applying buffer having pH 11 in the purification process with Fractogel®. The purified fractions were used for the determination of maximum loading. Fractogel® showed a six times higher loading capacity of  $291.5 \text{ mg}_{\text{protein}} \text{ g}_{\text{carrier}}^{-1}$  than the underivatized silica beads ( $54.3 \text{ mg}_{\text{protein}} \text{ g}_{\text{carrier}}^{-1}$ ). Difference in structure of both matrices could be responsible for different binding capacities.

Immobilization of the two enzymes *OsCGT* and *GmSuSy* capable for coupled nothofagin synthesis and simultaneously regeneration of the glycosyl-donor UDP-glucose was used to analyze the applicability of the affinity matrix. After setting up the silica beads with  $44 \text{ mg}_{\text{protein}} \text{ g}_{\text{carrier}}^{-1} Z_{\text{basic2-SAV}}$ , 200 µg of each enzyme were immobilized. The first of eight

consecutive reactions showed a 51 % conversion of phloretin to nothofagin at a reaction rate of  $67 \mu\text{M min}^{-1}$ . With increasing number of reactions, the conversion decreases to  $23 \mu\text{M min}^{-1}$  (34 % of initial reaction rate). The amount of UDP-glucose meanwhile increases from reaction to reaction, because of less consumption and probably leaching of enzymes (in particular *OsCGT*) leading to an unbalanced ratio of *GmSuSy* and *OsCGT*. Residual activity between 5 – 10 % of the carrier was found in the solution after separation of the carrier from reaction mix. The SDS-PAGE analysis of these fractions showed protein bands at the respective molecular weight of both enzymes, which is in line with the assumption that enzyme leaching causes reduced activity of the immobilized enzymes. *Z<sub>basic2</sub>-SAV* itself have not been identified in SDS-PAGE analysis implying relatively stable immobilization to the silica beads in the respective reaction environment.

Overall, *Z<sub>basic2</sub>-SAV* was successfully immobilized on Fractogel® and underivatized silica beads. On the obtained SAV affinity matrix based on silica beads *OsCGT* and *GmSuSy* were effectively bound and a conversion of phloretin to nothofagin was possible for multiple cycles. The loss of carrier activity of about 66 % in eight consecutive reactions was high and therefore binding via *streptag* II was too weak for the purpose of immobilization. Improvement of the SAV *strep-tag* II binding strength is key to use the herein described tandem enzyme immobilization. However, the observed binding strength is sufficient for the purification of strep-tagged protein, which could serve as an interesting alternative application.

## 6 References

- [1] Garcia-Galan, C., Berenguer-Murcia, Á., Fernandez-Lafuente, R., Rodrigues, R. C. (2011): Potential of Different Enzyme Immobilization Strategies to Improve Enzyme Performance. *Adv. Synth. Catal.*, 353, p. 2885–2904, DOI: 10.1002/adsc.201100534.
- [2] Barbosa, O., Ortiz, C., Berenguer-Murcia, Á., Torres, R., Rodrigues, R. C., Fernandez-Lafuente, R. (2015): Strategies for the one-step immobilization-purification of enzymes as industrial biocatalysts. *Biotechnology advances*, 33, p. 435–456, DOI: 10.1016/j.biotechadv.2015.03.006.
- [3] Sheldon, R. A., van Pelt, S. (2013): Enzyme immobilisation in biocatalysis: why, what and how. *Chemical Society reviews*, 42, p. 6223–6235, DOI: 10.1039/c3cs60075k.
- [4] Torres-Salas, P., del Monte-Martinez, A., Cutiño-Avila, B., Rodriguez-Colinas, B., Alcalde, M., Ballesteros, A. O., Plou, F. J. (2011): Immobilized Biocatalysts: Novel Approaches and Tools for Binding Enzymes to Supports. *Adv. Mater.*, 23, p. 5275–5282, DOI: 10.1002/adma.201101821.
- [5] Tran, D. N., Balkus, K. J. (2011): Perspective of Recent Progress in Immobilization of Enzymes. *ACS Catal.*, 1, p. 956–968, DOI: 10.1021/cs200124a.
- [6] Wiesbauer, J., Bolivar, J. M., Mueller, M., Schiller, M., Nidetzky, B. (2011): Oriented Immobilization of Enzymes Made Fit for Applied Biocatalysis: Non-Covalent Attachment to Anionic Supports using Zbasic2 Module. *ChemCatChem*, 3, p. 1299–1303, DOI: 10.1002/cctc.201100103.
- [7] Green, N. M. (1990): Avidin and streptavidin. *Methods in enzymology*, p. 51–67, DOI: 10.1016/0076-6879(90)84259-J.

- [8] Laitinen, O. H., Nordlund, H. R., Hytönen, V. P., Kulomaa, M. S. (2007): Brave new (strept)avidins in biotechnology. *Trends in biotechnology*, 25, p. 269–277, DOI: 10.1016/j.tibtech.2007.04.001.
- [9] Urh, M., Simpson, D., Zhao, K. (2009): Affinity Chromatography: General Methods. *Methods in enzymology*, 463, p. 417–438, DOI: 10.1016/S0076-6879(09)63026-3.
- [10] Wu, S.-C., Wang, C., Hansen, D., Wong, S.-L. (2017): A simple approach for preparation of affinity matrices: Simultaneous purification and reversible immobilization of a streptavidin mutein to agarose matrix. *Scientific reports*, 7, p. 42849, DOI: 10.1038/srep42849.
- [11] Wu, S.-C., Wang, C., Chin, J., Wong, S.-L. (2019): A bio-coupling approach using a dextran-binding domain to immobilize an engineered streptavidin to Sephadex for easy preparation of affinity matrix. *Scientific reports*, 9, p. 3359, DOI: 10.1038/s41598-019-40044-4.
- [12] Johar, S. S., Talbert, J. N. (2017): Strep-tag II fusion technology for the modification and immobilization of lipase B from *Candida antarctica* (CALB). *Journal, genetic engineering & biotechnology*, 15, p. 359–367, DOI: 10.1016/j.jgeb.2017.06.011.
- [13] Bolivar, J. M., Nidetzky, B. (2012): Positively charged mini-protein Zbasic2 as a highly efficient silica binding module: opportunities for enzyme immobilization on unmodified silica supports. *Langmuir the ACS journal of surfaces and colloids*, 28, p. 10040–10049, DOI: 10.1021/la3012348.
- [14] Bolivar, J. M., Schelch, S., Mayr, T., Nidetzky, B. (2015): Mesoporous Silica Materials Labeled for Optical Oxygen Sensing and Their Application to Development of a Silica-Supported Oxidoreductase Biocatalyst. *ACS Catal.*, 5, p. 5984–5993, DOI: 10.1021/acscatal.5b01601.

- [15] Gräslund, T., Lundin, G., Uhlen, M., Nygren, P.-A., Hober, S. (2000): Charge engineering of a protein domain to allow efficient ion-exchange recovery. *Protein engineering*, 13, p. 703–709.
- [16] Bolivar, J. M., Nidetzky, B. (2012): Oriented and selective enzyme immobilization on functionalized silica carrier using the cationic binding module Z basic2: design of a heterogeneous D-amino acid oxidase catalyst on porous glass. *Biotechnology and bioengineering*, 109, p. 1490–1498, DOI: 10.1002/bit.24423.
- [17] Humbert, N., Schürmann, P., Zocchi, A., Neuhaus, J.-M., Ward, T. R. (2008): High-Yield Production and Purification of Recombinant T7-Tag Mature Streptavidin in Glucose-Stressed *E. coli*. In: McMahon R.J. (eds) *Avidin-Biotin Interactions. Methods in Molecular Biology*, 418, p. 101–110, DOI: 10.1007/978-1-59745-579-4\_9.
- [18] Schmidt, T. G., Skerra, A. (1994): One-step affinity purification of bacterially produced proteins by means of the “Strep tag” and immobilized recombinant streptavidin. *Journal of chromatography. A*, 676, p. 337–345, DOI: 10.1016/0021-9673(94)80434-6.
- [19] Sano, T., Cantor, C. R. (1990): Expression of a cloned streptavidin gene in *Escherichia coli*. *Proceedings of the National Academy of Sciences of the United States of America*, 87, p. 142–146, DOI: 10.1073/pnas.87.1.142.
- [20] Studier, F. W. (1991): Use of Bacteriophage T7 Lysozyme to Improve an Inducible T7 Expression System. *Journal of molecular biology*, 219, p. 37–44, DOI: 10.1016/0022-2836(91)90855-Z.
- [21] Skerra, A., Voss, S. (1997): Mutagenesis of a flexible loop in streptavidin leads to higher affinity for the Strep-tag II peptide and improved performance in recombinant protein purification. *Protein engineering*, 10 (8), p. 975–982, DOI: 10.1093/protein/10.8.975.

- [22] Choi, J. H., Lee, S. Y. (2004): Secretory and extracellular production of recombinant proteins using *Escherichia coli*. *Applied microbiology and biotechnology*, 64, p. 625–635, DOI: 10.1007/s00253-004-1559-9.
- [23] Hendrickson, W. A., Pähler, A., Smith, J. L., Satow, Y., Merritt, E. A., Phizackerley, R. P. (1989): Crystal structure of core streptavidin determined from multiwavelength anomalous diffraction of synchrotron radiation. *Proceedings of the National Academy of Sciences of the United States of America*, 86, p. 2190–2194.
- [24] Schmidt, Thomas G M, Skerra, A. (2007): The Strep-tag system for one-step purification and high-affinity detection or capturing of proteins. *Nature protocols*, 2, p. 1528–1535, DOI: 10.1038/nprot.2007.209.
- [25] González, M., Argaraña, C. E., Fidelio, G. D. (1999): Extremely high thermal stability of streptavidin and avidin upon biotin binding. *Biomolecular Engineering*, 16, p. 67–72, DOI: 10.1016/S1050-3862(99)00041-8.
- [26] Schmidt, T. G. M. et al. (1996): Molecular Interaction Between the Strep-tag Affinity Peptide and its Cognate Target, Streptavidin. *Journal of molecular biology*, 255, p. 753–766.
- [27] Bungaruang, L., Gutmann, A., Nidetzky, B. (2013): Leloir Glycosyltransferases and Natural Product Glycosylation: Biocatalytic Synthesis of the C-Glucoside Nothofagin, a Major Antioxidant of Redbush Herbal Tea. *Advanced Synthesis & Catalysis*, 355, p. 2757–2763, DOI: 10.1002/adsc.201300251.
- [28] Bungaruang, L., Gutmann, A., Nidetzky, B. (2016):  $\beta$ -Cyclodextrin Improves Solubility and Enzymatic C -Glucosylation of the Flavonoid Phloretin. *Adv. Synth. Catal.*, 358, p. 486–493, DOI: 10.1002/adsc.201500838.
- [29] Gräslund, T., Hedhammar, M., Uhlén, M., Nygren, P.-A., Hober, S. (2002): Integrated strategy for selective expanded bed ion-exchange adsorption and site-specific protein

processing using gene fusion technology. *Journal of biotechnology*, *96*, p. 93–102, DOI: 10.1016/S0168-1656(02)00040-8.

[30] Lemmerer, M., Schmölzer, K., Gutmann, A., Nidetzky, B. (2016): Downstream Processing of Nucleoside-Diphospho-Sugars from Sucrose Synthase Reaction Mixtures at Decreased Solvent Consumption. *Advanced Synthesis & Catalysis*, *358*, p. 3113–3122, DOI: 10.1002/adsc.201600540.

[31] Müller, J. M., Wetzels, D., Flaschel, E., Friehs, K., Risse, J. M. (2016): Constitutive production and efficient secretion of soluble full-length streptavidin by an *Escherichia coli* 'leaky mutant'. *Journal of biotechnology*, *221*, p. 91–100, DOI: 10.1016/j.jbiotec.2016.01.032.

[32] Laitinen, O. H., Hytönen, V. P., Nordlund, H. R., Kulomaa, M. S. (2006): Genetically engineered avidins and streptavidins. *Cellular and molecular life sciences CMLS*, *63*, p. 2992–3017, DOI: 10.1007/s00018-006-6288-z.

[33] Gasteiger, E., Gattiker, A., Hoogland, C., Ivanyi, I., Appel, R. D., Bairoch, A. (2003): ExPASy: The proteomics server for in-depth protein knowledge and analysis. *Nucleic acids research*, *31*, p. 3784–3788, DOI: 10.1093/nar/gkg563.

[34] Weber, P. C., Wendoloski J. J. M., Pantoliano, M. W., F. R. Salemme (1992): Crystallographic and thermodynamic comparison of natural and synthetic ligands bound to streptavidin. *Journal of the American Chemical Society*, *114*, p. 3197–3200, DOI: 10.1021/ja00035a004.

[35] Schmidt, T., Skerra, A. (2015): The Strep-tag system for one-step affinity purification of proteins from mammalian cell culture. *Methods in molecular biology*, *1286*, p. 83–95, DOI: 10.1007/978-1-4939-2447-9\_8.

[36] Reznik, G. O., Vajda, S., Cantor, C. R., Sano, T. (2001): A Streptavidin Mutant Useful for Directed Immobilization on Solid Surfaces. *Bioconjugate chemistry*, *12*, p. 1000–1004, DOI: 10.1021/bc015507t.

- [37] Müller, J. M., Risse, J. M., Friehs, K., Flaschel, E. (2015): Model-based development of an assay for the rapid detection of biotin-blocked binding sites of streptavidin. *Engineering in Life Sciences*, 15, p. 627–639, DOI: 10.1002/elsc.201400227.
- [38] Kada, G., Falk, H., Gruber, H. J. (1999): Accurate measurement of avidin and streptavidin in crude biofluids with a new, optimized biotin–fluorescein conjugate. *Biochimica et Biophysica Acta (BBA) - General Subjects*, 1427, p. 33–43, DOI: 10.1016/S0304-4165(98)00178-0.
- [39] Bolivar, J. M., Gascon, V., Marquez-Alvarez C., Blanco R. M., Nidetzky, B. (2017): Oriented Co-immobilization of Oxidase and Catalase On Tailormade Ordered Mesoporous Silica. *Langmuir The ACS journal of fundamental interface science*, 33, p. 5065-5076, DOI: 10.1021/acs.langmuir.7b00441
- [40] Bolivar, J. M., Luley-Goedl, C., Leitner, E., Sawangwan, T., Nidetzky, B. (2017): Production of glucosyl glycerol by immobilized sucrose phosphorylase: Options for enzyme fixation on a solid support and application in microscale flow format. *Journal of biotechnology*, 257, p. 131–138, DOI: 10.1016/j.jbiotec.2017.01.019
- [41] Zong, C., Duic, B., Bolivar, J. M., Nidetzky, B. (2020): Three-Enzyme Phosphorylase Cascade Immobilized on Solid Support for Biocatalytic Synthesis of Cello-oligosaccharides. *ChemCatChem*, 12, p. 1350–1358, DOI: 10.1002/cctc.201901964
- [42] Valikhani, D., Bolivar, J. M., Denning, A., Nidetzky, B. (2018): A tailor-made, self-sufficient and recyclable monooxygenase catalyst based on coimmobilized cytochrome P450 BM3 and glucose dehydrogenase. *Biotechnology and Bioengineering*, 115, p. 2416-2425, DOI: 10.1002/bit.26802.

## 7 Appendix

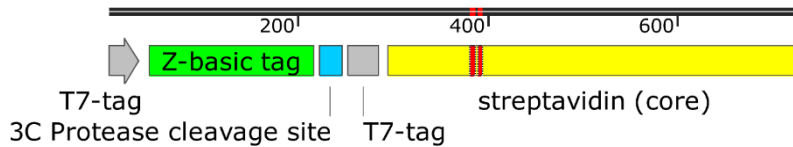


**Fig. 7-1: Schematic representation of the recombinant gene  $Z_{\text{basic2-SAV}}$ .** Coding regions are marked in grey and core streptavidin mutation introduced by Skerra et al. are marked in red [21].

$Z_{\text{basic2-SAV}}$  (729 bp) 5'-3'

```

1 ATGGCTAGCA TGACTGGTGG ACAGCAAATG GGTCGCGGAT CCGTAGACAA
51 CAAATTCAAC AAAGAACGTC GCCGTGCTCG CCGTGAAATC CGTCACTTAC
101 CTAACTTAAA CCGTGAACAA CGCCGTGCTT TCATTTCGTT CCTGCGTGAT
151 GACCCAAGCC AAAGCGCTAA CTTGCTAGCA GAAGCTAAAA AGCTAAATGA
201 TGCTCAGGCG CCGAAACCGA ATTTGGAAGC TCTGTTCCAG GGTCCGAATT
251 CTATGGCTAG TATGACGGGC GGTCAACAAA TGGGTCGCGA TCAAGCGGGT
301 ATCACGGGCA CCTGGTATAA TCAACTGGGC TCCACCTTCA TTGTTACCGC
351 AGGTGCTGAT GGTGCACTGA CCGGCACGTA TGTCACGGCG CGTGGTAACG
401 CCGAATCCCG CTATGTGCTG ACCGGTCGTT ATGATTCAGC CCCGGCAACC
451 GATGGTAGCG GTACCGCACT GGGTTGGACC GTTGCCTGGA AAAACAATTA
501 TCGCAATGCA CATAGTGCTA CCACCTGGTC CGGCCAGTAT GTCGGCGGTG
551 CAGAAGCTCG TATTAACACG CAATGGCTGC TGACCAGCGG CACCACGGAA
601 GCGAATGCCT GGAAATCTAC CCTGGTGGGT CACGATACCT TTACGAAAGT
651 TAAACCGAGC GCGGCCTCTA TCGACCCGC TAAAAAAGCA GGTGTCAACA
701 ATGGTAACCC GCTGGATGCC GTTCAACAG

```

**Fig. 7-2 : Sequence of  $Z_{\text{basic2-SAV}}$**

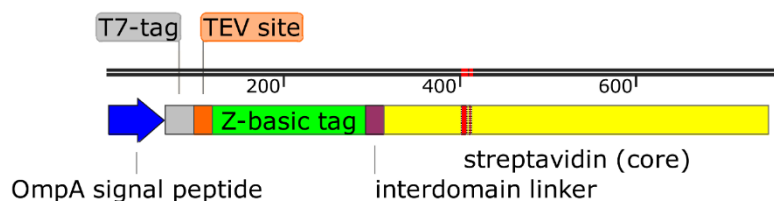


**Fig. 7-3: Schematic representation of the recombinant gene  $OmpA-Z_{\text{basic2-SAV}}$ .** Core streptavidin mutation introduced by Skerra et al. are marked in red [21]. The gene was cloned in the pET-26b(+) vector using *Nde*I and *Xho*I restriction sites by GenScript.

OmpA-Zbasic2-SAV (762 bp) 5'-3'

```

1 ATGAAGAAAA CAGCTATAGC AATAGCTGTA GCACTAGCTG GATTTGCTAC
51 TGTTCGCGCAG GCGATGGCGA GCATGACCGG CGGCCAACAG ATGGGCGAGA
101 ACCTGTACTT CCAAGGTGTG GACAACAAGT TTAACAAAGA GCGTCGTCGT
151 GCGCGTCGTG AAATCCGTCA CCTGCCGAAC CTGAACCGTG AGCAGCGTCG
201 TCGTTCATT CGTAGCCTGC GTGACGATCC GAGCCAAAGC GCGAACCTGC
251 TGGCGGAAGC GAAGAACTG AACGATGCGC AGGCGCCGAA GGGTAGCGGT
301 AGCGGTAGCG GTGCGGGTAT CACCGGCACC TGGTACAACC AACTGGGTAG
351 CACCTTTATT GTTACCGCGG GTGCGGATGG TGCCTGACC GGTACCTATG
401 TGACCGCGCG TGGTAACGCG GAAAGCCGTT ACGTTCTGAC CGGCCGTTAT
451 GACAGCGCGC CGGCGACCGA TGGTAGCGGT ACCGCGCTGG GTTGGACCGT
501 GCGGTGGAAG AACAACTACC GTAACGCGCA CAGCGCGACC ACCTGGAGCG
551 GCCAGTATGT TGGTGGCGCG GAGGCGCGTA TCAACACCCA ATGGCTGCTG
601 ACCAGCGGCA CCACCGAAGC GAACGCGTGG AAAAGCACCC TGGTGGGTCA
651 CGATACCTTC ACCAAGGTTA AACCGAGCGC GCGGAGCATT GATGCGGCGA
701 AGAAGGCGGG CGTGAATAAC GGTAATCCGC TGGACGCGGT TCAACAGTAA
751 TGA CTCGAG

```

Fig. 7-4 : Amino acid sequence of OmpA-Z<sub>basic2</sub>-SAV

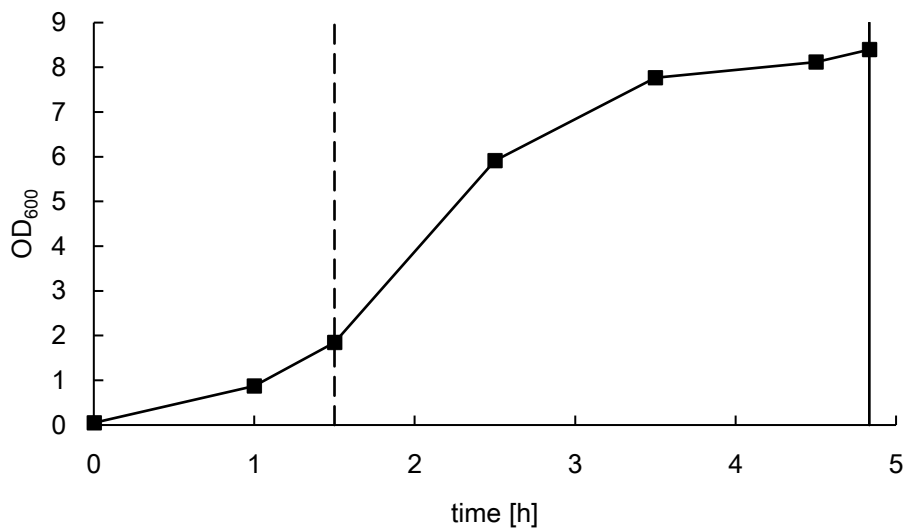


Fig. 7-5 Growth curve of *E. coli*/BL21(DE3)/pLysS in 2 L bioreactor. 1.8 L of MTP media were autoclaved and 60 µg mL<sup>-1</sup> kanamycin and 34 µg mL<sup>-1</sup> chloramphenicol were added. 40.7 mL of preculture were mixed with 40 mL of 20 % w/v glucose. The expression was induced by addition of 0.4 mM IPTG at an OD<sub>600</sub> of 1.85 (dashed line). The cells were harvested after 3 h and 20 min by centrifugation for 30 min at 5000 g at 4 °C (line).

**Tab. 7-1: Raw data for the determination of maximum loading of Z<sub>basic2</sub>-SAV on Fractogel®.** C<sub>protein</sub> protein concentration (N=2); V<sub>fraction</sub> fraction volume; m<sub>x</sub> protein mass; yield<sub>immo</sub> immobilization yield relative immobilized protein amount to maximum loading.

fraction	C <sub>protein 1</sub> [mg mL <sup>-1</sup> ]	C <sub>protein 2</sub> [mg mL <sup>-1</sup> ]	V <sub>fraction</sub> [mL]	m <sub>sup protein</sub> [mg]	m <sub>offered protein</sub> [mg]	m <sub>immobilized</sub> [mg]	C <sub>protein/carrier</sub> [mg g <sup>-1</sup> ]	yield <sub>immo</sub> [%]
S1	0.46	0.46	1.00	0.46	2.85	2.39	207.65	71.24
S2	1.84	1.84	1.00	1.84	2.85	3.40	295.40	101.34
S3	2.57	2.54	1.00	2.56	2.85	3.70	321.03	110.13
S4	2.67	2.72	1.00	2.70	2.85	3.85	334.49	114.75
$\sum^{protein}$				7.55	11.40			
W1	0.31	0.33	1.00	0.32				
W2	0.13	0.11	1.00	0.12				
W3	0.05	0.06	1.00	0.06				
$\sum^{protein}$				0.50				

**Tab. 7-2: Raw data for the determination of maximum loading of Z<sub>basic2</sub>-SAV on underivatized silica beads.** C<sub>protein</sub> protein concentration (N=2); V<sub>fraction</sub> fraction volume; m<sub>x</sub> mass; yield<sub>immo</sub> immobilization yield relative immobilized protein amount to maximum loading.

fraction	C <sub>protein 1</sub> [mg mL <sup>-1</sup> ]	C <sub>protein 2</sub> [mg mL <sup>-1</sup> ]	V <sub>fraction</sub> [mL]	m <sub>total protein</sub> [mg]	m <sub>offered protein</sub> [mg]	m <sub>immobilized</sub> [mg]	C <sub>protein/carrier</sub> [mg g <sup>-1</sup> ]	yield <sub>immo</sub> [%]
S1	0.03	0.03	0.50	0.02	0.53	0.52	9.94	18.30
S2	0.05	0.05	0.50	0.03	0.53	1.02	19.69	36.25
S3	0.35	0.36	0.50	0.18	0.53	1.37	26.50	48.78
S4	0.12	0.12	0.50	0.06	0.53	1.84	35.57	65.49
S5	0.40	0.40	0.40	0.16	0.83	2.51	48.50	89.30
S6	0.80	0.80	0.40	0.32	0.83	3.02	58.35	107.43
S7	1.39	1.32	0.40	0.56	0.87	3.33	64.30	118.38
S8	1.88	1.88	0.40	0.75	0.80	3.38	65.22	120.08
$\sum^{protein}$				2.07	5.45			
W1	0.33	0.34	1.00	0.34				
W2	0.13	0.13	1.00	0.13				
W3	0.10	0.10	1.00	0.10				
W4	0	0	1.00	0				
$\sum^{protein}$				0.57				

**Tab. 7-3: Raw data for multiple nothofagin synthesis cycles with immobilized *OsCGT* and *GmSuSy* on *Z<sub>basic2</sub>*-SAV-silica beads support.** Consecutive reactions 1-8 were started by addition of reaction solution to the catalyst. After 15 min of incubation the catalyst was separated and an additional sample A-G was taken after 15 min. The data were acquired with HPLC in a single run with extended reversed-phase ion-pairing method [30].

sample	total area				relative area [%]				Canalyte [mM]			
	UDP-glc	UDP	nothofagin	phloretin	UDP-glc	UDP	nothofagin	phloretin	UDP-glc	UDP	nothofagin	phloretin
blank	0.0	40.7	0.0	494.7	0.0	100.0	0.0	100.0	0.00	0.25	0.00	2.00
blank	0.0	43.2	0.0	555.3	0.0	100.0	0.0	100.0	0.00	0.25	0.00	2.00
1	6.3	45.7	347.2	328.1	12.1	87.9	51.4	48.6	0.03	0.22	1.03	0.97
2	19.2	110.4	573.8	653.0	14.8	85.2	46.8	53.2	0.04	0.21	0.94	1.06
3	13.4	56.0	336.7	610.7	19.3	80.7	35.5	64.5	0.05	0.20	0.71	1.29
4	15.0	52.6	268.1	690.6	22.2	77.8	28.0	72.0	0.06	0.19	0.56	1.44
5	18.9	54.1	255.2	822.0	25.9	74.1	23.7	76.3	0.06	0.19	0.47	1.53
6	24.0	49.7	204.9	806.3	32.6	67.4	20.3	79.7	0.08	0.17	0.41	1.59
7	32.0	55.7	186.6	900.9	36.5	63.5	17.2	82.8	0.09	0.16	0.34	1.66
8	29.2	55.6	247.3	828.5	34.4	65.6	23.0	77.0	0.09	0.16	0.46	1.54
A	6.3	72.4	627.7	436.4	8.0	92.0	59.0	41.0	0.02	0.23	1.18	0.82
B	7.0	89.3	651.6	658.6	7.3	92.7	49.7	50.3	0.02	0.23	0.99	1.01
C	8.1	106.1	552.0	843.6	7.1	92.9	39.6	60.4	0.02	0.23	0.79	1.21
D	9.5	95.0	394.8	922.5	9.1	90.9	30.0	70.0	0.02	0.23	0.60	1.40
E	13.9	97.9	320.1	972.0	12.4	87.6	24.8	75.2	0.03	0.22	0.50	1.50
F	18.6	94.5	300.4	1054.0	16.4	83.6	22.2	77.8	0.04	0.21	0.44	1.56
G	21.9	90.4	265.7	1052.9	19.5	80.5	20.2	79.8	0.05	0.20	0.40	1.60